HHS Public Access

Author manuscript

Cell Rep. Author manuscript; available in PMC 2025 May 13.

Published in final edited form as:

Cell Rep. 2025 April 22; 44(4): 115527. doi:10.1016/j.celrep.2025.115527.

Dietary oleic acid drives obesogenic adipogenesis via modulation of LXRα signaling

Allison Wing[1], **Elise Jeffery**[2,10], **Christopher D. Church**[3,10], **Jennifer Goodell**[3], **Rocío del M. Saavedra-Peña**[1], **Moumita Saha**[3], **Brandon Holtrup**[1], **Maud Voisin**[4], **N. Sima Alavi**[3], **Mariana Floody**[3], **Zenan Wang**[1], **Thomas E. Zapadka**[5], **Michael J. Garabedian**[4,6], **Rohan Varshney**[7], **Michael C. Rudolph**[7,*], **Matthew S. Rodeheffer**[1,2,8,9,11,*]

[1]Department of Molecular, Cell, and Developmental Biology, Yale University, 219 Prospect St., New Haven, CT 06520, USA

[2]Department of Cell Biology, Yale University School of Medicine, 333 Cedar St., New Haven, CT 06520, USA

[3]Department of Comparative Medicine, Yale University School of Medicine, 310 Cedar St., New Haven, CT 06520, USA

[4]Department of Microbiology, NYU School of Medicine, New York, NY 10016, USA

[5]Department of Cellular and Molecular Physiology, Yale University School of Medicine, New Haven, CT 06520, USA

[6]Department of Medicine, NYU School of Medicine, New York, NY 10016, USA

*Correspondence: michael-rudolph@ouhsc.edu (M.C.R.), matthew.rodeheffer@yale.edu (M.S.R.).

AUTHOR CONTRIBUTIONS

Conceptualization, A.W., E.J., and M.S.R.; methodology, A.W., E.J., M.J.G., M.C.R., and M.S.R.; software, A.W., R.d.M.S.-P., and Z.W.; investigation, A.W., E.J., R.d.M.S.-P., M.S.R., M.C.R., Z.W., C.D.C., J.G., B.H., T.E.Z., and M.V.; resources, M.J.G.; writing – original draft, A.W. and E.J.; writing – review & editing, A.W., M.C.R., R.V., M.J.G., and M.S.R.; visualization, A.W., E.J., and M.S.R.; supervision, M.S.R.

RESOURCE AVAILABILITY

Lead contact

Requests for additional information, resources, or reagents should be addressed and will be executed by the lead contact, Matthew S. Rodeheffer (matthew.rodeheffer@yale.edu).

Materials availability

LXR S196A is available from the providing institution. All other reagents are commercially available.

Data and code availability

- RNA-seq data were deposited with GEO. Data from male and female APCs are under accession numbers GEO: GSE273569 and GSE209663, respectively. Data from 3T3-L1 cells are under accession number GEO: GSE273735. All other data in this paper will be shared by the lead contact upon request.
- There is no original code reported in this publication.
- Any additional information required to reanalyze the data reported in this paper is available from the lead contact upon request.

DECLARATION OF INTERESTS

The authors declare no conflicts of interest.

SUPPLEMENTAL INFORMATION

Supplemental information can be found online at 10.1016/j.celrep.2025.115527.

[7]Department of Biochemistry and Physiology and Harold Hamm Diabetes Center, Oklahoma University Health Sciences, Oklahoma City, OK 73104, USA

[8]Yale Stem Cell Center, Yale University School of Medicine, 10 Amistad St., New Haven, CT 06520, USA

[9]Yale Center of Molecular and Systems Metabolism, Yale University School of Medicine, New Haven, CT 06520, USA

[10]These authors contributed equally

[11]Lead contact

SUMMARY

Dietary fat composition has changed substantially during the obesity epidemic. As adipocyte hyperplasia is a major mechanism of adipose expansion, we aim to ascertain how dietary fats affect adipogenesis during obesity. We employ an unbiased dietary screen to identify oleic acid (OA) as the only dietary fatty acid that induces obesogenic hyperplasia at physiologic levels and show that plasma monounsaturated fatty acids (MUFAs), which are mostly OA, are associated with human obesity. OA stimulates adipogenesis in mouse and human adipocyte precursor cells (APCs) by increasing AKT2 signaling, a hallmark of obesogenic hyperplasia, and reducing LXR activity. High OA consumption decreases LXRα Ser196 phosphorylation in APCs, while blocking LXRα phosphorylation results in APC hyperproliferation. As OA is increasingly being incorporated into dietary fats due to purported health benefits, our finding that OA is a unique physiologic regulator of adipose biology underscores the importance of understanding how high OA consumption affects metabolic health.

Graphical Abstract

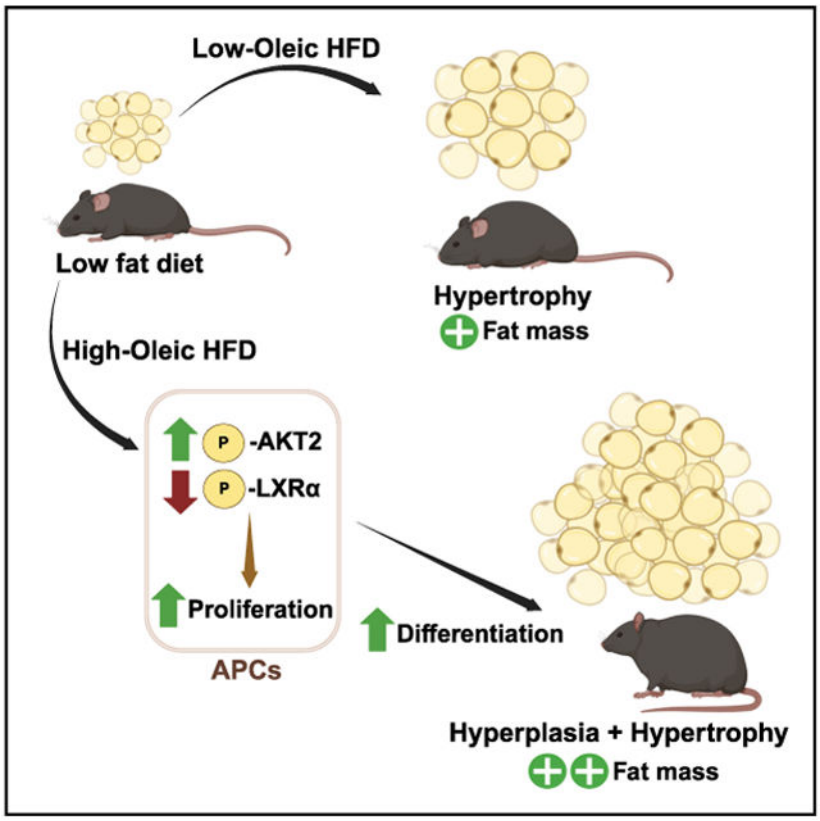

In brief

Wing et al. identify dietary oleic acid (OA) as a driver of adipogenesis during obesity through AKT2 signaling and decreased LXRα activity. This increased fat cell formation contributes to long-term fat mass and highlights the importance of understanding the effects of high OA levels in diet.

INTRODUCTION

The obesity epidemic is the result of a complex interplay between genetic and environmental factors. While associations between obesity and positive energy balance have been established,[1-3] increased obesity rates have also coincided with significant changes in dietary composition, whose effects on adipose biology require further understanding. While the impact of dietary sugars on obesity and metabolic disease has been extensively studied,[4] the effect of modern dietary fat composition has received less attention. Although overall fat intake increased marginally during the onset of the obesity epidemic,[5] the dietary fat source has been altered substantially,[5-7] which has even resulted in modification of the fatty acid composition of triglycerides stored in human adipose.[8] Given the coincidence of these changes in dietary fat with the onset of the obesity epidemic, we aimed to understand how variations in dietary fat composition impact obesogenic adipose expansion and weight gain.

During obesity, adipose tissue expansion and weight gain are driven by an increase in adipocyte number (hyperplasia) and an increase in adipocyte size (hypertrophy).[9,10]

While changes in hypertrophy can occur relatively rapidly and are reversible,[11,12] adipose hyperplasia is persistent due to the long lifespan of adipocytes[13,14] and, thus, may contribute to interminable weight retention.[14] We and others have shown that the mechanisms driving adipocyte hyperplasia are distinct from the mechanisms that establish adipocyte number during development.[15,16] Therefore, elucidating the mechanisms that regulate obesogenic adipocyte hyperplasia is important for understanding the factors that drive sustained increases in fat mass during obesity.

Adipocytes form via the proliferation and subsequent differentiation of adipocyte precursor cells (APCs).[16,17] In mice, a high-fat diet (HFD) activates APCs, inducing a transient burst of proliferation during the first week of HFD consumption. These activated APCs differentiate and accumulate lipids to form mature adipocytes, contributing to increased fat mass.[18] This obesogenic hyperplasia requires AKT2 signaling, which distinguishes HFD-induced adipogenesis from the establishment of adipose tissue during development.[15] However, the identity of the diet-derived signal that stimulates AKT2 signaling in APCs remains unknown. Since certain fatty acids can function as bioactive signaling molecules[19,20] and previous studies of obesogenic hyperplasia primarily utilized lard-based HFDs, we sought to determine if dietary fatty acid composition affects obesogenic hyperplasia. Here, we show that dietary oleic acid (OA) is a necessary dietary obesogenic signal for driving HFD-induced adipogenesis. We further show that OA regulates liver X receptor (LXR) activity during the initiation of obesogenic hyperplasia and that APC proliferation is modulated by the phosphorylation at S196 of LXRα.

RESULTS

Dietary fat composition modulates obesogenic adipogenesis

HFD feeding results in increased caloric consumption[21,22] and altered circadian food intake, which are both associated with obesity.[23] To determine whether obesogenic activation of APCs is due to increased caloric intake, mice were pair-fed HFD to calorically match mice fed a standard diet (SD) for 1 week. APC proliferation was then quantified using flow cytometry and previously established markers identifying APCs (Figure S1A).[15] In the pair-fed mice, the HFD significantly increased epididymal white adipose tissue (EWAT) APC proliferation compared to the SD (Figure 1A), despite the pair-fed mice consuming an equivalent number of calories as control mice. To determine if altered circadian feeding impacts obesogenic APC activation, we assessed APC proliferation in mice that were fed *ad libitum* or restricted to nighttime or daytime feeding only. The HFD increased EWAT APC proliferation compared toSD in mice fed either *ad libitum* or with time-restricted feeding regimens (Figure S1B). These results indicate that HFD-induced APC activation is not driven by increased caloric intake or altered feeding patterns associated with HFDs, suggesting that diet composition dictates APC activation upon high-fat feeding.

To assess if the dietary fat source determines APC proliferation, mice were fed commercially available HFDs (Table S1) with different fat sources for 1 week, and APC proliferation was quantified. Mice fed the 45% and 60% kcal lard and 43% kcal milkfat HFDs demonstrated increased EWAT APC proliferation compared to mice fed the SD. Mice fed the 58% coconut oil diets containing either cornstarch (CS) or sucrose (Suc)

as the carbohydrate source did not have increased APC proliferation compared to mice fed the SD, despite their substantial fat content (Figure 1B). Of note, there was no significant difference in subcutaneous white adipose tissue (SWAT) APC proliferation on any of the diets, consistent with the depot-specific patterning of obesogenic APC activation in male mice (Figure 1C).[15] To determine if diets that induce APC proliferation also promote differentiation, we used the adiponectin-CreER mTmG (AdiER) mouse model to quantify *in vivo* adipogenesis, as previously described.[15] This system employs a dual-color fluorescent reporter. Initially, all cells display red membrane fluorescence due to the expression of membrane-targeted dTomato. Upon administration of tamoxifen, Cre recombinase expression is induced in adipocytes. This Cre expression triggers an irreversible genetic switch, causing these cells to switch from dTomato expression to GFP expression. The result is a permanent transition from red to green fluorescence, specifically in the mature adipocytes that express the tamoxifen-inducible Cre recombinase (Cre-ER [estrogen receptor]) at the time of tamoxifen treatment. Mice were treated with tamoxifen, followed by a recovery period, and then fed different diets. We observed significantly more EWAT adipocyte formation in mice fed a lard-based HFD compared to the coconut-oil-based-HFD- and SD-fed mice. In contrast, the coconut HFD did not increase adipocyte formation compared to the SD, while SWAT adipogenesis was unchanged in all diets (Figures 1D and 1E). To further quantify the effect of dietary fats on adipocyte formation, we performed a BrdU pulse-chase experiment where mice were given BrdU in drinking water during the first week of the diet, which labels proliferating APCs, followed by a 7-week chase in the absence of BrdU. After 8 weeks of diet consumption, EWAT was examined for BrdU-labeled adipocyte nuclei to score mature adipocytes that formed from cells that proliferated during the first week of the diet switch. The lard HFD increased mature adipocyte formation compared to SD- and coconut-HFD-fed mice, which were not different (Figure 1F). These results suggest that the type of dietary fat is a critical determinant of obesogenic hyperplasia.

To evaluate how differences in adipose hyperplasia impact long-term fat mass, mice were fed the SD, lard HFD, or coconut HFD for 20 weeks. Quantification of adipocyte hypertrophy indicated that adipocyte size distribution was similar between mice consuming the coconut-oil- and lard-based diets (Figure 1G). Despite similar adipocyte size distributions, EWAT mass was significantly increased in mice on the lard diet, suggesting that the adipocyte hyperplasia induced by the lard HFD resulted in long-term fat mass accumulation (Figure 1H). These results demonstrate that adipose hyperplasia is modulated by diets with different fat compositions, with significant impacts on long-term obesity.

OA is a diet-derived driver of APC proliferation

While these results using commercially available HFDs suggest that the source of dietary fat modulates APC proliferation, adipogenesis, and obesity, these diets were not matched in fat quantity and contained variations in carbohydrate and protein composition, which could affect adipogenesis. To isolate the role of dietary fats on adipose hyperplasia, we designed a series of isocaloric 45% kcal fat diets, which are identical except for the source of fat (Figure S1C and Table S1). Mice were fed these diets for 1 week along with drinking water containing BrdU to quantify APC proliferation. After 1 week on the different diets, EWAT APCs exhibited a range of proliferative responses to the HFDs, with some diets, such

as fish and palm oil, inducing no significant change in APC proliferation, while soybean, high-oleic (HO) sunflower, HO safflower, and peanut significantly increased proliferation (Figure 2A). Consistent with previous findings in male mice, subcutaneous WAT (SWAT) APC proliferation did not significantly increase on any of the diets. These data establish that, when controlling for macronutrient contributions, carbohydrate sources, and caloric content, the dietary fat source regulates APC proliferation.

To assess how the dietary fat source affects adipogenesis, diets were fed to the AdiER mouse model for 8 weeks. In addition to increased APC proliferation, the lard, olive, soybean, and HO safflower diets also significantly increased EWAT adipocyte formation compared to the SD (Figures 2B and 2C). However, the HO sunflower and peanut diets, which induced the highest APC proliferation, resulted in lower rates of adipogenesis and were not significantly greater than the SD. Additionally, consistent with the APC proliferation data, SWAT adipocyte formation was much lower than EWAT and displayed less variation in response to the dietary fat source. These data suggest that dietary fat modulates both APC proliferation and differentiation and potentially influences precursor fate.

One possible mechanism by which OA may influence obesogenic adipogenesis is via insulin signaling, as insulin plays a direct role in adipogenesis.[25] Furthermore, insulin secretion is augmented by certain fatty acids,[26,27] and insulin is a well-known driver of AKT2 phosphorylation,[28,29] which is required for obesogenic adipogenesis.[15] Therefore, we next evaluated whether changes in circulating insulin are associated with diet-driven adipogenesis. Mice were fed the complete diet screen for 3 days, which is the peak of HFD-induced APC proliferation,[15] and plasma insulin was quantified from non-fasted mice. Fed plasma insulin in the different HFDs demonstrated no correlation to EWAT APC proliferation (Figure S1D) or adipocyte hyperplasia (Figure S1E). In addition, HFD feeding stimulates phosphorylation of AKT2 in SWAT APCs (Figure S1F), similar to EWAT,[15] despite the lack of adipogenic response to the HFD in male SWAT. Thus, while AKT2 signaling is a necessary component of obesogenic adipogenesis, it is not sufficient. Therefore, it is unlikely that dietary fat composition regulates adipogenesis through changes in insulin signaling alone.

To understand how dietary fat impacts adipose hyperplasia, fatty acid mass spectrometry analysis was performed to quantify the fatty acid composition of each diet. Of the dietary fatty acids, OA was the only fatty acid present in all diets that significantly correlated with EWAT APC proliferation (Figure 2D; Table 1). This relationship contrasted with other abundant dietary fatty acids, such as 16:0, 18:0, and 18:2n-6, which do not associate with APC activation. We next tested the correlation of dietary OA to APC proliferation via two different approaches. First, mice were fed an SD supplemented with triglyceride containing only OA (tri-oleate) to 45% kcal fat, matching the custom diet series. When mice were fed this diet for 1 week, the tri-oleate diet was sufficient to increase EWAT APC proliferation (Figure 2E). Next, we fed mice an SD supplemented to 45% kcal with either stearic acid (18:0), OA (18:1), or linoleic acid (18:2). Of these diets, only the OA-enriched diet induced EWAT APC proliferation, while stearic and linoleic acid diets did not increase APC proliferation (Figure 2F).

We next determined how dietary fat composition affects plasma fatty acids. Total fatty acids and OA were quantified in plasma over time as mice adapted to HFD consumption. The plasma levels of total fatty acids and OA peaked on day 3 and decreased on day 7 (Figures 2G, 2H, and Table S2). This pattern mimics the previously determined pattern of APC proliferation, which also peaks on day 3 of HFD consumption and subsides by day 7,[15] supporting an association between diet-derived OA and APC proliferation. In the diet screen, the plasma levels of many fatty acids relate to their dietary levels. While this includes essential fatty acids, as expected, it also includes non-essential fatty acids, including palmitate and OA (Table S3). Furthermore, APC proliferation positively correlates to plasma OA (Figure S1G and Table S4) and monounsaturated fatty acids (MUFAs), which are mostly comprised of OA (Table S5). While APC proliferation also negatively correlates to plasma 8:0 and 16:2, 8:0 was only present in one diet, and 16:2 was not detected in any of the diets. These results show that APC proliferation is linked to plasma OA concentrations, which are influenced by OA consumption.

To determine if increased plasma OA is sufficient to drive APC proliferation, OA was administered directly into the blood stream via a jugular catheter. This method of OA delivery significantly increased plasma OA (Figure S1H) and increased EWAT APC proliferation (Figure 2I). These data establish that dietary OA increases plasma OA, thereby stimulating APC proliferation *in vivo*.

Finally, to determine whether plasma fatty acids are related to human obesity, we consulted available data from the UK Biobank, which includes quantification of 249 plasma biomarkers from 500,000 participants living in the UK.[24,30] In examining hazard ratios for participants diagnosed as obese or overweight, we found that percent MUFA in plasma exhibited the highest hazard ratio of the metabolites measured (Figure 2J). Given that OA is the major MUFA in plasma and diet, these results suggest that OA consumption plays a role in human obesity.

OA-driven adipogenesis requires AKT2 signaling

To determine if OA affects APCs directly, we established the effects of fatty acids on primary APC differentiation *in vitro*. Primary APCs were isolated from lean mice and cultured *in vitro*, followed by induction of adipogenesis using insulin alone, an adipogenic cocktail of insulin, dexamethasone, and 3-isobutyl-1-methylxanthine (MDI), or insulin alone supplemented with a panel of individual fatty acids. Of the fatty acids screened, only OA (C18:1) and palmitoleic acid (C16:1) significantly increased lipid accumulation compared to insulin-only controls (Figure 3A). Cells were treated with 100 μM of each fatty acid, which is a physiologic level of OA but a hyperphysiologic level for plasma palmitoleic acid, which is less than 10 μM[31,32] (Table S2). These data suggest that OA is the only fatty acid that is a physiologic driver of adipogenesis. Finally, to determine whether OA also increases adipogenesis in human APCs, primary APCs were harvested from human adipose samples and differentiated with or without OA. OA robustly increased lipid accumulation in human APCs compared to controls (Figure 3B). Taken together, these data suggest that OA increases APC differentiation in both mice and humans.

Next, we sought to identify the OA-stimulated pathways involved in obesogenic adipogenesis. AKT2 signaling is a hallmark of obesogenic adipogenesis, distinguishing this process from hyperplasia during the establishment of adipose during normal development.[15] First, flow cytometry on day 3 of diet treatment showed that a low-OA HFD (coconut oil) does not stimulate AKT2 phosphorylation at Ser473 in EWAT APCs (Figure S2A), which indicates that high dietary fat consumption is not sufficient to activate AKT2 signaling. To determine if OA activates AKT2, we quantified AKT2 phosphorylation in OA-treated primary APCs. After 3 h of differentiation, OA supplementation significantly increased Ser473 phosphorylation compared to insulin alone (Figures 3C, 3D, and S2B-S2D).

We then determined if AKT2 is required for OA-induced differentiation using *Akt2*$^{-/-}$ primary APCs differentiated with MDI, insulin, or insulin supplemented with OA. While there was no difference in adipogenesis between wild-type (WT) and *Akt2*$^{-/-}$ APCs when treated with insulin alone or MDI, *Akt2*$^{-/-}$ APCs showed decreased differentiation relative to WT when treated with OA, indicating that OA-enhanced adipogenesis occurs through AKT2 signaling (Figure 3E). In addition, OA treatment induced adipocyte markers, such as *Pparγ*, *Cebpα*, *Adipoq*, *Fabp4*, and *Plin*, in WT APCs but not in *Akt2*$^{-/-}$ APCs (Figure 3F), further supporting that OA-stimulated adipogenesis requires AKT2. Finally, to quantify the *in vivo* impact of AKT2 signaling on diet-induced APC proliferation, WT and *Akt2*$^{-/-}$ mice were fed either an SD or an SD supplemented with OA to 45% kcal fat. The OA-supplemented diet stimulated EWAT APC proliferation in WT mice but not in *Akt2*$^{-/-}$ mice (Figure 3G). There was no difference in SWAT APC proliferation in either WT or *Akt2*$^{-/-}$ mice fed the OA-supplemented diet (Figure S2E). These data show that OA-induced proliferation and differentiation are dependent on AKT2 signaling in APCs, linking OA to the known mechanism of obesogenic hyperplasia *in vivo*.

LXR signaling and phosphorylation inhibit diet-driven APC proliferation

One potential mechanism of OA-enhanced APC proliferation is signaling through free fatty acid receptors. Gpr120 and Gpr40 bind to medium- and long-chain fatty acids, and Gpr120 has been implicated in adipose hyperplasia.[33-35] To establish whether either of these receptors is responsible for OA-induced APC proliferation, Gpr120 knockout (Gpr120KO)[36] and Gpr40KO[37] mice were fed a 60% lard HFD for 1 week with BrdU treatment. Both KO models demonstrated a significant increase in APC proliferation in response to HFD compared to SD controls (Figure S3A), indicating that these receptors are not required for OA stimulation of APC proliferation.

To assess how dietary OA activates APCs, we performed RNA sequencing (RNA-seq) on APCs sorted from mice fed a 60% kcal lard HFD for 3 days, when APC proliferation peaks.[15] To identify pathways related to diet-induced hyperplasia, we took advantage of the fact that APCs of female mice proliferate in both in both EWAT and SWAT in response to HFD.[18] Thus, we scrutinized pathways that were common between the hyperplastic tissues (female SWAT and EWAT and male EWAT) and not affected in male SWAT. Of these pathways, the downregulation of LXR/retinoid X receptor (RXR) activation was of particular interest given its ability to regulate cell proliferation[38] and the role of LXR in lipogenesis and adipogenesis[39] (Figure 4A). While *Lxrα* is highly expressed in APCs, there

was no significant change in *Lxrα* expression in the APCs of HFD-fed mice (Figure S3B). However, an analysis of LXR activity in 3T3L1 cells transfected with a luciferase LXR reporter construct demonstrated that OA downregulates LXR transcriptional activity, while the LXR agonist T0901317 (T0) increased activity (Figure 4B). Given that LXRα, and not LXRβ, interacts with fatty acids,[40] these data support that OA acts via LXRα in adipogenic cells.

To examine how LXR activation impacts adipogenesis, 3T3-L1 cells were differentiated with MDI or MDI supplemented with OA or OA and T0. OA induced differential expression of 195 genes relative to MDI control (Figure 4C). Consistent with its role in APC activation, the top pathways affected by OA treatment included cell-cycle- and checkpoint-regulated pathways (Figure S3C). Importantly, LXR agonist T0 restored most OA-regulated genes and pathways (Figures 4C and S3D), which supports that LXR is a major effector of OA in adipogenesis. As LXRα is a central regulator of lipogenesis,[41] we further analyzed the effect of OA on lipogenic genes involved in OA synthesis. OA treatment dramatically decreased two stearoyl-coenzyme A desaturases (*Scd*), *Scd1* and *Scd2* expression (Figure 4D), with no effect on the expression of *Srebp1* or the other lipogenic genes, *Elovl6*, *Fasn*, or *Acc1* (Figure S3E). This downregulation of the stearoyl desaturases was reversed with the addition of T0. As *Scd1* and *Scd2* catalyze the rate-limiting step in OA synthesis,[42] these data suggest that OA feedback does not generally affect lipogenesis but rather specifically targets its own synthesis via the downregulation of LXRα-mediated expression of stearoyl desaturases.

To determine how LXR activity impacts adipogenesis, primary APCs were treated *in vitro* with insulin or insulin supplemented with OA or OA and T0. While OA increased lipid accumulation during differentiation, the addition of T0 decreased adipogenesis relative to OA treatment alone (Figure 4E). Finally, to assess how LXR activation impacts diet-induced APC activation *in vivo*, mice were fed a 60% lard HFD for 3 days and treated with vehicle or T0. While the HFD increased EWAT APC proliferation, T0 treatment inhibited this activation (Figure 4F), suggesting that downregulation of LXR activity is required for HFD-induced APC proliferation.

Modulation of LXRα by phosphorylation at Ser196 influences metabolic disease and gene expression programs.[43] To determine if LXRα phosphorylation in APCs is altered by the high-OA HFD, immunohistochemistry was performed on EWAT sections from mice fed a 60% lard HFD for 3 days. Sections were co-stained for Sca1 to identify APCs and phospho-Ser196-LXRα. HFD feeding decreased the proportion of $Sca1^+$ APCs with phosphorylated LXRα (Figures 4G and 4H). We then further characterized the role of LXRα phosphorylation on APC proliferation using mice harboring a point mutation of Ser196 to alanine (S196A) to block this site of LXRα phosphorylation.[44] Upon being fed a 60% lard HFD, these mice showed increased EWAT APC proliferation compared to the APCs of WT mice (Figure 4I). Thus, blocking LXRα phosphorylation results in APC hyperproliferation in response to an HFD. Taken together, these data suggest that OA induces APC proliferation by decreasing LXRα phosphorylation at Ser196.

Lxra is expressed in a wide variety of tissues and other cell types within adipose tissue,[45,46] and therefore, the APC hyperproliferation in the point mutation mice could be due to effects from other cells or tissues. To determine whether increased APC activation is due to the regulation of LXRα phosphorylation within APCs, we performed an APC transplant experiment, as described previously.[18,47] In brief, dTomato+ APCs were harvested from either WT mTmG mice or mTmG mice possessing the S196A point mutation. The donor APCs were transplanted into the EWAT of a WT recipient mouse, which then received 3 days of a 60% lard HFD and BrdU (Figures 4J and S3F). From these mice, APC proliferation was compared between endogenous, non-fluorescent cells and transplanted, RFP+ cells (Figure 4K). Similar to whole-body point mutation mice, transplanted S196A APCs had significantly greater APC proliferation compared to endogenous cells and transplanted WT cells, indicating that the inhibition of high-OA-HFD-induced APC proliferation by LXRα phosphorylation is cell autonomous.

DISCUSSION

While the molecular mechanisms of adipogenesis are well characterized *in vitro,*[48-50] obesogenic adipogenesis is a distinct process[15] whose *in vivo* molecular regulators have not been defined. We developed an unbiased screen to assess the role of dietary fatty acids as physiologic drivers of adipogenesis. Dietary OA is the only fatty acid that positively associates with obesogenic adipogenesis and induces obesogenic APC proliferation *in vivo* and differentiation at physiologically relevant levels. Furthermore, we show that OA regulates obesogenic hyperplasia via altered phosphorylation and regulation of LXRα function in APCs. Broadly, this study supports the concept that dietary fat composition impacts physiology by regulating specific signaling pathways. Moreover, it demonstrates that even highly abundant dietary fatty acids, often viewed solely as sources of energy, can act as bioactive compounds. The results show that our HFD screen is an effective, well-controlled tool with sufficient power to deconvolute the complex effects of dietary fatty acids on physiology, and the interactions discovered can be leveraged to identify underlying cellular and molecular mechanisms.

Our results indicate that LXRα is central to the physiologic response to OA. LXRα is a fatty-acid-responsive nuclear receptor[40] that regulates the expression of lipid-regulatory genes, including those involved in cholesterol transport,[51] cholesterol metabolism,[52] and initiation of lipogenesis.[53] The regulation of LXRα transcriptional activity is complex. LXRs have several endogenous ligands, which induce disparate functional responses.[54] Diet is an additional regulatory mechanism, with a high-cholesterol diet changing the availability of LXR ligands,[52,55,56] leading to changes in the gene expression program of LXR.[57] In addition, the phosphorylation status of LXRα selectively regulates transcription activity.[43] These selective regulatory mechanisms could explain the contradictory results from previous studies on the role of LXRα in adipogenesis,[39,58-60] as the contribution of LXRα to adipogenesis likely depends on the specific adipogenic conditions, whether in culture or *in vivo*. Our data identify OA as an important diet-derived adipogenic mediator, which is facilitated by LXRα dephosphorylation rather than LXRα expression. Given the intricacy of LXRα signaling,[57] blocking LXRα phosphorylation via the S196A mouse model provides a more targeted approach and reveals more about the underlying signaling mechanisms

compared to an LXRα knockdown model. However, further work is needed to define the mechanisms by which OA affects LXRα activity.

We identify OA as the sole dietary driver of APC proliferation through the association of dietary fatty acid composition in the HFD screen, direct infusion into the bloodstream via catheter, and directed dietary supplementation. This identification of OA as a physiologic regulator is consistent with previous work showing interactions between LXRα and OA. OA downregulates LXRα activity in HEK293 cells in culture[40,61] and during acute respiratory distress in the lung.[62] LXRα also mediates the physiologic effects of OA in hepatic lipogenesis, with broad induction of lipogenic genes, including *Scd1* and *Scd2*.[63] However, regulation of gene expression by LXR in adipose tissue is highly divergent from that of liver,[64,65] and we show that in the adipogenic lineage, OA selectively downregulates stearoyl desaturases (Figure 4D), which are the enzymes required to generate OA *in vivo*. As LXRα directly regulates the expression of stearoyl-coenzyme A desaturases (SCDs),[66] these data indicate that OA serves as a classic metabolic feedback inhibitor of its own production in APCs via modulation of LXR function through regulating LXRα phosphorylation.

Despite the clear effect of OA on LXR function, how OA influences LXRα activity remains unknown, including whether its impact depends on OA uptake. Free OA can bind to LXRα,[61] indicating that direct regulation is possible, potentially by affecting ligand binding, coregulator interaction, or recognition by kinases or phosphatases. OA could also affect LXR indirectly by regulating pathways responsible for LXRα phosphorylation, such as the kinases creatine kinase 2 (CK2),[43] protein kinase A (PKA),[67] and PCKα.[68] OA may also affect APC function via incorporation into other bioactive lipid species. For example, phospholipid composition is highly responsive to dietary lipid content,[69] and LXR facilitates fatty acid incorporation into phospholipids.[70] As alterations in membrane composition can modulate cell proliferation,[71,72] OA incorporation into membrane lipids could also influence obesogenic adipogenesis. While dietary OA is clearly associated with hyperplastic adipose expansion in obesity, further work is needed to define the molecular mechanisms involved.

We link LXRα to obesogenic adipocyte hyperplasia, which we have previously shown requires AKT2[15] and ERα signaling.[18,47] In females, obesogenic hyperplasia occurs in both visceral and subcutaneous adipose.[18] In males, this process is normally restricted to EWAT, but SWAT APC proliferation is stimulated when estrogen treatment is combined with an HFD.[18] Here, we show that a high-OA HFD increases AKT2 signaling in male SWAT APCs, despite this depot lacking APC proliferation, but that a low-OA HFD does not stimulate AKT2 phosphorylation in EWAT. These data indicate that OA stimulates AKT2 activation along with modulation of LXRα function, but AKT2 activation alone is not sufficient to drive hyperplasia. Thus, for effective adipocyte hyperplasia in females and male SWAT, OA modulation of LXRα and AKT2 likely requires estrogen signaling via ERα. Given that male visceral adipose can also produce estrogen,[73,74] it is possible that estrogen signaling is also required in normal male adipocyte hyperplasia. Notably, these three pathways also interact in breast cancer,[75-78] with ERα acting both upstream and downstream of AKT2.[79] Further work is required to determine how these three signaling mechanisms interact to control adipocyte hyperplasia in obesity.

While we demonstrate that OA produces signaling effects that lead to adipocyte hyperplasia and increased fat mass, the impact of adipocyte hyperplasia on metabolic health remains unclear. Several genetic and pharmacologic mouse models with high levels of adipogenesis are metabolically healthy.[80-84] Thus, increased adipose hyperplasia may safely expand storage capacity in the adipose tissue, limiting lipid spillover into liver and muscle, thereby reducing insulin resistance and glucose intolerance.[82-84] In this framework, the associations of dietary OA with improvements in health[85-87] may be linked to OA-induced adipogenesis. However, excess OA is associated with increased mortality and cardiovascular risk.[88,89] In this case, long-term OA-driven obesogenic hyperplasia may contribute to increased fat mass and ultimately be detrimental to metabolic health. These contradictions are also observed in humans, where relatively short-term studies show an improvement in lipoprotein profiles with a HO diet compared to control diets despite increased visceral adipose mass.[90] This effect on fat mass is consistent with our data showing that OA increases adipogenesis in human and mouse APCs and with the finding that plasma MUFAs have a high hazard ratio for obesity in humans.

The contrasting effects of OA on health could be due to the dietary dose of OA. Studies using relatively low levels of dietary OA show beneficial effects, while higher levels of OA consumption have been shown to have detrimental effects on cardiovascular health and mortality.[91] This point is important to consider, as many factors have led to drastic changes in the fat composition of the food supply over the last several decades.[92] These include the development of technologies to produce palatable oils from plant sources[93] and efforts to reduce dietary saturated and *trans* fats in diets.[94] More recently, plant oils with high levels of OA are being developed and introduced into foods for numerous reasons, including the premise that dietary OA is healthy.[95,96] However, the efficacy of any beneficial agent depends on its appropriate dosage. Our work indicates that at high levels, dietary OA functions as a unique signaling molecule relative to other fatty acids and drives long-term effects on fat mass via a dose-dependent promotion of adipogenesis. Recent FDA guidelines uphold high levels of dietary OA as beneficial,[97] and several common food oils, such as soybean and canola, that have been modified to increase OA levels above 70% are now becoming more prevalent in the food supply.[98] As our findings show that high levels of dietary OA stimulate adipogenesis and that plasma MUFA levels are associated with human obesity, it is important that future work deconvolute the role of OA and other dietary fatty acids in weight management, metabolic signaling, health, and disease.

Limitations of the study

Dietary OA will signal in tissues throughout the body, making it difficult to isolate the metabolic consequences of diet-induced adipogenesis. Currently, genetic models that accurately and specifically target APCs are not available[99]; therefore, our ability to determine the effect of obesogenic adipogenesis on systemic metabolism is currently limited. While the whole-body point mutation demonstrated a robust increase in APC proliferation during HFD feeding, this mutant is known to have effects in other tissues and cells types, and even the adoptive transfer of LXRα-S196A hematopoietic cells in a WT background has been shown to indirectly impact adipose mass.[100] While our APC transplant model presents a well-controlled opportunity to observe the effects of APC-intrinsic LXRα

phosphorylation on APC proliferation, the relatively small quantity of transplanted cells that are commonly generated in tissue progenitor cell transplant studies precludes analysis of the effects on systemic metabolism in this model.

Another limitation in studies of dietary fats is that it is currently not possible to selectively remove an individual fatty acid from a fat source. Also, as dietary fat sources are a complex mixture of fatty acids mostly contained at varying positions in triglycerides, the generation of a synthetic dietary fat source that accurately reconstitutes an available fat source, such as lard, is not feasible. Thus, a synthetic diet approach to produce dietary fat sources that lack an individual fatty acid is not a viable approach. Thus, our conclusions on the role of dietary OA *in vivo* rely on the association of OA to APC proliferation from the HFD screen and specific effects of OA when it is added to the diet.

STAR★METHODS

EXPERIMENTAL MODEL AND SUBJECT DETAILS

Mice: All experiments using animals were conducted according to guidelines by Yale University's Institutional Animal Care and Use Committee (IACUC). Mice were group-housed in temperature and humidity-controlled rooms with a 12h light/dark cycle. All mice were on a C57BL/6J background, with the exception of Gpr120$^{-/-}$, which were C57BL/6N. Wild-type animals purchased from Jackson Laboratories. Adiponectin-CreER/mTmG mice were bred in in the Yale Animal Resource Center from Adiponectin-CreER mice gifted by E. Rosen (RRID:IMSR_JAX:024671; Beth Israel Deaconess Medical Center, Boston, MA, USA) and mTmG B6.129 (Cg)-Gt(ROSA) 26Sortm4(ACTB-tdTomato,-EGFP)Luo/J purchased from Jackson Laboratories (RRID: IMSR_JAX007676). Atk2$^{-/-}$ mice were a kind gift from William Sessa (RRID: IMSR_0006966; Yale University, New Haven, CT, USA). LXRα S196A mice for the three-day HFD experiment were housed at New York University, and fixed cells were kindly provided by Michael Garabedian. LXRα S196A/mTmG mice were bred at Yale University. Gpr40$^{-/-}$ were provided by Vincent Poitout (RRID: MGI:3713765; University of Montreal, Montreal, Quebec, Canada), and Gpr120$^{-/-}$ mice were provided by Jan Oscarsson (AstraZeneca, Gothenburg, Sweden). Unless otherwise noted, experiments were started using mice aged 6–8 weeks old. These studies focus on male mice, as adipocyte hyperplasia is known to have different depot patterning in the sexes and is affected by endogenous estrogen levels in females.[18,47] Experimental groups were randomly selected based on male littermates, if they were bred in house, or by cage, if they were purchased by Jackson Laboratory. We use the terms EWAT to refer to the perigonadal visceral adipose tissue and SWAT to refer to the inguinal subcutaneous adipose tissue.

Standard diet (SD) was purchased from Harlan Laboratories (2018S). The 60% lard-based diet and 58% kcal Coconut-based diet were purchased from Research Diets, Inc. Tri-oleate or fatty acids were added to SD to 45% kcal fat. For *in vivo* infusion experiments, jugular catheters were implanted into the right vein when mice were 8 weeks old. Oleic acid (20 mM) or vehicle (0.5% fatty acid free BSA in saline) were infused just before the dark cycle for 5 days. The 45% kcal HFDs were purchased from Research Diets, Inc. For the pair feeding experiment, SD and HFD groups were offset by one day. The kcal of SD consumed

on the previous day was calculated and the HFD pair-fed mice were then restricted to an equivalent kcal of SD from the previous day.

For *in vivo* BrdU experiments lasting one week, mice were given 0.8 mg/mL BrdU in drinking water with fresh solution made every other day. For BrdU pulse-chase experiments, BrdU was administered at 0.4 mg/mL in drinking water for one week and then removed and normal water provided.

To treat mice with T0901317, mice were given conditioning injections using medium chain triglycerides (MCT) daily for 4 days. Mice were then given MCT or 50 mg/kg of T0901317 daily for 3 days along with HFD before being sacrificed and processed for BrdU analysis.

Cells: All cells were cultured at 37°C with 5% CO_2 and saturating humidity and were maintained in growth media consisting of DMEM supplemented with 1% penicillin/streptomycin and 10% fetal bovine serum. 3T3-L1 (RRID: CVCL-0123) cells are derived from fibroblasts of a male mouse embryo. They were purchased from ATCC and tested negative for mycoplasma but were not authenticated. 3T3-L1 cells were passaged every 2–3 days. Primary APCs were harvested from SWAT of male mice and maintained under the same culture conditions.

Human subjects: Consent and experimental protocols to isolate human APCs were reviewed and approved by the Yale Internal Review board (HIC protocol number 1109009063). Samples were subcutaneous and abdominal adipose tissue regarded as waste materials from bariatric surgeries or elective abdominoplasties. Samples were stored in sterile saline solution until processing. APCs were isolated from five samples and were divided between treatments depending on cell yield.

METHOD DETAILS

Adiponectin-CreER/mTmG pulse-chase experiment: This experiment was performed as previously described.[15] At 8 weeks of age, Adiponectin-CreER/mTmG mice were given daily injections of tamoxifen in vegetable oil at 50 mg/kg for 5 days. The mice were then given a week to recover and then were fed the indicated diet for 8 weeks. At the end of 8 weeks, the mice were sacrificed, and their SWAT and EWAT were mounted on slides. The tissues were imaged using confocal microscopy, and the percentage of red adipocytes was quantified.

Microscopy: For the BrdU pulse-chase and adipocyte sizing experiments, adipose tissue was dissected and prepared for paraffin embedding as described.[105] Tissues were dissected and fixed in zinc formalin for 24–48 h. The tissues were then washed twice in PBS and incubated overnight in 70% ethanol. The tissues were then incubated in 75%, 95%, and 100% ethanol, and Citrisolv. The tissues incubated in melted paraffin before being embedded. Paraffin blocks were sectioned by Yale Pathology Tissue Services.

To quantify BrdU during the pulse-chase experiment, tissue sections were deparaffinized, and antigens were retrieved under pressure in a citrate solution. Samples were incubated in 2% BSA block solution for 1 h. They were then incubated in rat anti-BrdU and rabbit

anti-caveolin antibody at 4°C overnight and washed. Sections were incubated in anti-rat Alexa Fluor 488 and anti-rabbit Rhodamine-X-Red for 2 h and washed. Finally, sections were mounted using DAPI mounting media and imaged. Adipocyte nuclei were identified by their location within the adipocyte membrane.

For adipocyte sizing, tissue sections were stained with Masson's Trichrome stain or caveolin and imaged using a Zeiss microscope. To quantify adipocytes sizes, sections were systemically imaged and processed using a CellProfiler[101] pipeline adapted from a previous publication.[105] At least 300 adipocytes were quantified from each mouse.

To quantify phospho-LXRα in APCs, sections were deparaffinized as described. After blocking with 2% BSA in PBS, cells were incubated overnight with rat anti-Sca1 and rabbit anti-phospho- LXRα at 4°C. Sections were washed and incubated with donkey anti-rat Alexa Fluor 647 for 2 h at room temperature. Sections were then washed three times in PBS. Tyramide SuperBoost Kit Alex Fluor 594 was used to augment the phospho-LXRα signal. Sections were incubated with poly-HRP-conjugated secondary antibody at room temperature for 1 h. They were then washed three times with PBS and incubated with tyramide working solution for 5 min at room temperature. Sections were washed three times with PBS when incubated at room temperature with DAPI for 15 min. They were then washed three times with PBS and mounted for imaging.

Plasma insulin quantification: Mice were fed the HFD series for 3 days. In the morning, whole blood was collected from fed mice via tail nick using heparinized capillary tubes and was centrifuged at 8000 g for 8 min at 4°C to collect plasma. Samples were stored at −20°C until analysis. Insulin was quantified by ELISA according to the manufacturer instructions (ALPCO).

Flow cytometry: Flow cytometry for analysis, isolation of APCs, and BrdU quantification were performed as previously described.[15,106] Adipose tissue was dissected, minced, and digested using a 0.8 mg/mL collagenase II dissolved in 3% BSA in Hank's Balanced Salt Solution (HBSS). Cells were sequentially filtered 40 μm filter, with a prior 100 μm filtration step if the cells were being sorted. If cells were being analyzed or sorted, they were stained using antibodies for CD45, CD31, CD29, CD34, Sca1, and CD24 (concentrations in key resources table). Cells were analyzed using a BD LSRII analyser and BD FACS Diva software.

If the cells were being analyzed for BrdU quantification, they were pre-stained with antibodies for CD45, CD31, CD29, and Sca1. Cells were then washed, fixed, and permeabilized according to the instructions for Phosflow Lyse/Fix and Perm Buffer III. Cells were then treated with Dnase in PBS and washed with 3% BSA in HBSS. The cells were incubated with the BrdU antibody overnight, washed, then stained a mixture of antibodies for CD45, CD31, CD29, CD34, Sca1, and CD24. They were analyzed using a BD LSYII analyser and BD FACS Diva software.

Mean fluorescent intensity of phosphorylated AKT was measured as previously described.[15] APCs were harvested, lysed and fixed as described for the above but with all buffers

containing Roche PhosStop phosphatase inhibitor cocktail and 15 μM wortmannin. APCs were incubated at 4°C with phospho-AKT S473 antibody overnight.

To quantify proliferation in LXRα S196A mice, Ki67 was used as a marker of proliferation. To quantify Ki67 in APCs, WAT was digested and incubated in Phosflow Lyse/Fix as discussed for the BrdU quantification. Cells were then washed twice in Intracellular Staining Permeabilization Wash Buffer. After washing, cells were incubated with Anti-Ki67 FITC. Cells were washed twice again in Permeabilization Wash buffer and resuspended in 3% BSA in HBSS for analysis.

Isolation of human APCs: Tissues were washed with Krebs Ringer Phosphate (KRP) solution containing 0.8 mM $ZnCl_2$, 1 mM $MgCl_2$, and 1.2 mM $CaCl_2$. Tissues were minced, washed in KRP solution, and centrifuged to separate red blood cells. Samples were then digested in KRP solution with 3% FBS and collagenase type II for 75 min in a shaking water bath at 37°C. Samples were then filtered and washed with KRP and 3% chelexed fetal calf serum (FCS). The floating layer of adipocytes was removed. Stromal vascular fraction was then incubated with GP38-PE antibody for 15 min. Cells were then washed with buffer (KRP with 3% chelexed FCS) and incubated with EasySep PE Selection Cocktail and then with EasySep Magnetic Nanoparticles. The tube was then placed in a magnet, and supernatant was poured off. Captured cells were then resuspended in buffer.

Biomarker associations: Association plot was accessed from the Biomarker-Wide Association Plots available from Nightingale Health.[24] Methods of sample processing and association have been previously described.[30] In brief, plasma was harvested at baseline from 500,000 participants of the UK Biobank (as of date of access). 249 plasma biomarkers were quantified by nuclear magnetic resonance as performed by Nightingale Health laboratories. Biomarkers associations were identified via logistic regression and were adjusted for sex, assessment center, and age.

Cell transplant assay: Cell transplants were performed as previously described.[18] SWAT and EWAT APCs were harvested and pooled from several mice as detailed above. APCs were rinsed and resuspended in PBS. Recipient mice were anesthetized with Isothesia when aged 4 weeks old. At least 0.5 million APCs were injected into the tip of one recipient EWAT depot. Recipient mice were allowed to recover for 2 weeks and then placed on HFD for 1 week. They were then sacrificed and analyzed for BrdU incorporation into APCs.

***In vitro* adipogenesis assay and Oil Red O staining:** To differentiate primary APCs, upon reaching confluence, media was not changed for 48 h. Media was then supplemented with 0.1 μg/mL insulin and maintained in this solution for 7 days with media changings every other day. If cells were being differentiated in the presence of a fatty acid, the fatty acid was conjugated to fatty acid free BSA and added to the differentiation media at 100 μM.

3T3-L1 cells were differentiated with an adipocyte cocktail (MDI) consisting of 0.1 μg/mL insulin, 30 μg/mL 3-isobutyl-1methylxantine, and 0.1 μg/mL dexamethasone. After 48 h, media was maintained in 0.1 μg/mL insulin and changed every other day for 7 days.

To quantify accumulated lipid, cells were washed twice with PBS and fixed in a solution containing 0.2% glutaraldehyde and 2% formaldehyde in PBS. The cells were then washed twice with PBS, twice with water, and briefly with 60% isopropanol. After the washes, the cells were stained with a mixture of 60% Oil Red O and 40% water and then washed briefly with 60% isopropanol and twice with water. The cells were imaged and left in water overnight. The next day, the cells were dried for several hours and then the stain was extracted using a solution of 4% NP40 in isopropanol. The absorbance of the extraction solution was then analyzed on a spectrophotometer at 500 nm.

Transfection and luciferase reporter assay: 3T3-L1 cells were cultured in a 48 well plate to nearly confluent before transfection. Cells were transfected using Lipofectamine 2000 Transfection Reagent in OptiMEM. Cells were transfected with Cignal LXR Reporter Kit (500 ng) for 24 h. Media was then changed to treatment media.

LXR activity was quantified using the Luciferase Assay System according to the protocol. Cells were lysed and spun at 12,000 g for 2 min at 4°C. Sample was then mixed with luciferase assay substrate, and luminescence was quantified over 10 s.

Real time qPCR: If analyzing tissue expression, tissues were dissected and frozen in liquid nitrogen and stored at −80°C. The tissues were then homogenized in Trizol. If analyzing cells, cells were washed in PBS and then suspended in Trizol Reagent. If not being processed immediately, the cells were frozen in Trizol at −80°C.

RNA from both tissues and cells was harvested using a Direct-zol RNA Miniprep kits and quantified using a nanodrop spectrophotometer. RNA was converted to cDNA using a reverse transcription kit. qPCR was performed with SYBR Green I Mastermix on a LightCycler 480 Real-Time PCR system. Genes were normalized to β-actin or *Ubc* as indicated, with primer sequences in Table S6.

Immunoblots: Primary APCs were lysed using 1% IGEPAL with protease and PhosStop phosphatase inhibitors. Protein was quantified using Pierce BCA protein assay kit. Protein was incubated with NuPage 2X Sample Buffer and Sample Reducing Agent. Western blots were run on 10% Bis-Tris gels. Protein was then transferred to PVDF membranes using the Invitrogen NuPage system.

Membranes were stained with rabbit anti-Akt2 or rabbit anti-phospho-Akt2 in tris-buffered saline with 0.1% Tween 20 (TBST). Membranes were then incubated with goat anti-rabbit-HRP secondary antibody and developed with SuperSignal West Pico Chemiluminescent Substrate.

Fatty acid mass spectrometry: Individual stable isotope fatty acid (FA) stock solutions were made in isooctane/ethyl acetate 3:1 v/v, for which a mixture containing 1.0 μg/μL of each FA was made. The isotope stock solution was further diluted to 50 ng/μL,for use as internal reference standards for each acyl chain length and saturation. FA regression curves were prepared, and GC/MS was conducted according to.[107,108] Briefly, plasma was collected at 0, 3, or 7 days or 12 weeks of diet consumption, and 10 μL was analyzed for

total FA composition. For plasma and rodent diets, 500 ng of the blended internal reference standard was added to 200 μL and 50 μL of total lipid extract, respectively, and samples were taken to dryness under N_2 gas. Dried samples were immediately resuspended in 500 μL of 100% ethanol, saponified with 500 μL of 1M NaOH at 90°C for 45 min in Teflon capped tubes and then acidified by addition of 525 μL pf 1M HCl. Saponified FA were re-extracted twice using 1 mL of isooctane, dried under N_2 gas, and were derivatized by sequential addition of 1% pentafluorobenzyl bromine and 1% diisopropylethylamine (in acetonitrile v/v) at RT for 30 min. The resulting pentafluorobenzyl FA esters were resuspended in 200 μL of isooctane and diluted 1:10 into isooctane into GC/MS autosampler vials for injection. Analyte data were acquired in NICI full scan, the FA-analyte peak area ratio to that of its corresponding stable isotope reference FA was calculated for each analyte, and ratios were converted to absolute amounts relative to regression curves for each chain length and saturation.[107,108] Quantitative FA data were normalized to the volume of plasma, total serum protein as determined by BCA assay, or the total mass of rodent diet, input to the lipid extraction.

RNA-sequencing: For RNAseq from APCs, data from female samples were obtained from Saavedra et al.,[47] while samples from males were collected in a similar manner. APCs were sorted from male and female mice fed SD or 60% lard HFD for 3 days as described above. For females, 3 mice were pooled for each sample with a total of 5 samples. Cells were lysed in TRIzol Reagent, and RNA was isolated. Samples were submitted to the Yale Center for Genome Analysis (YCGA). The mRNA library was prepared (polyA), and sequencing was conducted using HiSeq2500 single-end 1x75bp sequencing. Reads were aligned to mm9 using TopHat[102] and quantified using python module HTSeq[103] with preset parameters. Genes with fewer than 20 reads across all samples were filtered out. DEGs induced over SD were identified using DESeq2,[104] and DEGs were defined as $p < 0.01$ with absolute value of log-2-fold change >0.6.

For RNAseq from 3T3-L1 cells, cells were differentiated for 24 h with MDI, MDI with oleic acid, or MDI with 5μM T0901317. RNA was harvested, submitted for sequencing at YCGA, and analyzed as described above. DEGs were defined as $p < 0.05$ and absolute value of log-2-fold change >1.5.

QUANTIFICATION AND STATISTICAL ANALYSIS

Statistical tests for each experiment are described in associated figure legend. Data in graphs are presented as mean ± SEM, and sample number is indicated in each figure legend. The value n indicates individual animals for *in vivo* experiments and independent experiments for *in vitro* experiments. A *p*-value <0.05 was considered statistically significant and was indicated by asterisks (*$p < 0.05$, **$p < 0.01$, ***$p < 0.001$, ****$p < 0.0001$). Statistics were analyzed using DESeq2, R, and Ingenuity Pathway Analysis for RNA-seq data, and GraphPad Prism for all else.

Supplementary Material

Refer to Web version on PubMed Central for supplementary material.

ACKNOWLEDGMENTS

We thank Yale Flow Cytometry for their assistance with flow cytometry analyzers and FACS service, the Yale Center for Genomics Analysis for sequencing, and the Yale Comparative Medicine Pathology Core for histology preparation and staining. This work was supported by NIDDK grants DK090489 and DK126447 and the Naratil Pioneer Award from the Women's Health Research at Yale to M.S.R.; the National Science Foundation Graduate Research Fellowship (NSF-GRFP) and Ford Foundation Predoctoral Fellowship to R.d.M.S.-P.; Lo Fellowships for Excellence in Stem Cell Research to A.W. and E.J.; and an EMBO postdoctoral fellowship to C.D.C. The Yale Flow Core is supported in part by an NCI Cancer Center Support Grant, NIH P30 CA016359. The BD Symphony was funded by a shared instrument grant, NIH S10 OD026996. Sequencing analysis was supported by the National Institute of General Medical Sciences of the NIH under award no. 1S10OD030363-01A1. The graphical abstract was created using BioRender.

REFERENCES

1. Hall KD, Farooqi IS, Friedman JM, Klein S, Loos RJF, Mangelsdorf DJ, O'Rahilly S, Ravussin E, Redman LM, Ryan DH, et al. (2022). The energy balance model of obesity: beyond calories in, calories out. Am. J. Clin. Nutr 115, 1243–1254. 10.1093/ajcn/nqac031. [PubMed: 35134825]
2. Turnbaugh PJ, Ley RE, Mahowald MA, Magrini V, Mardis ER, and Gordon JI (2006). An obesity-associated gut microbiome with increased capacity for energy harvest. Nature 444, 1027–1031. 10.1038/nature05414. [PubMed: 17183312]
3. Schwartz MW, Seeley RJ, Zeltser LM, Drewnowski A, Ravussin E, Redman LM, and Leibel RL (2017). Obesity Pathogenesis: An Endocrine Society Scientific Statement. Endocr. Rev 38, 267–296. 10.1210/er.2017-00111. [PubMed: 28898979]
4. Huang Y, Chen Z, Chen B, Li J, Yuan X, Li J, Wang W, Dai T, Chen H, Wang Y, et al. (2023). Dietary sugar consumption and health: umbrella review. Bmj-Brit Med J 381, e071609. 10.1136/bmj-2022-071609.
5. Shan Z, Rehm CD, Rogers G, Ruan M, Wang DD, Hu FB, Mozaffarian D, Zhang FF, and Bhupathiraju SN (2019). Trends in Dietary Carbohydrate, Protein, and Fat Intake and Diet Quality Among US Adults, 1999-2016. JAMA 322, 1178–1187. 10.1001/jama.2019.13771. [PubMed: 31550032]
6. Crino M, Sacks G, Vandevijvere S, Swinburn B, and Neal B (2015). The Influence on Population Weight Gain and Obesity of the Macronutrient Composition and Energy Density of the Food Supply. Curr. Obes. Rep 4, 1–10. 10.1007/s13679-014-0134-7. [PubMed: 26627085]
7. Lee JH, Duster M, Roberts T, and Devinsky O (2021). United States Dietary Trends Since 1800: Lack of Association Between Saturated Fatty Acid Consumption and Non-communicable Diseases. Front. Nutr 8, 748847. 10.3389/fnut.2021.748847. [PubMed: 35118102]
8. Guyenet SJ, and Carlson SE (2015). Increase in adipose tissue linoleic acid of US adults in the last half century. Adv. Nutr 6, 660–664. 10.3945/an.115.009944. [PubMed: 26567191]
9. Faust IM, Johnson PR, Stern JS, and Hirsch J (1978). Diet-induced adipocyte number increase in adult rats: a new model of obesity. Am. J. Physiol 235, E279–E286. 10.1152/ajpendo.1978.235.3.E279. [PubMed: 696822]
10. Steinberg MD, Zingg W, and Angel A (1962). Studies of the number and volume of fat cells in adipose tissue. J. Pediatr 61, 299–300. 10.1016/s0022-3476(62)80282-0. [PubMed: 13916686]
11. Tang HN, Tang CY, Man XF, Tan SW, Guo Y, Tang J, Zhou CL, and Zhou HD (2017). Plasticity of adipose tissue in response to fasting and refeeding in male mice. Nutr. Metab 14, 3. 10.1186/s12986-016-0159-x.
12. Hansson B, Morén B, Fryklund C, Vliex L, Wasserstrom S, Albinsson S, Berger K, and Stenkula KG (2019). Adipose cell size changes are associated with a drastic actin remodeling. Sci. Rep 9, 12941. 10.1038/s41598-019-49418-0. [PubMed: 31506540]
13. Hirsch J, and Han PW (1969). Cellularity of Rat Adipose Tissue - Effects of Growth Starvation and Obesity. J. Lipid Res 10, 77–82. [PubMed: 5764119]
14. Spalding KL, Arner E, Westermark PO, Bernard S, Buchholz BA, Bergmann O, Blomqvist L, Hoffstedt J, Näslund E, Britton T, et al. (2008). Dynamics of fat cell turnover in humans. Nature 453, 783–787. 10.1038/nature06902. [PubMed: 18454136]

15. Jeffery E, Church CD, Holtrup B, Colman L, and Rodeheffer MS (2015). Rapid depot-specific activation of adipocyte precursor cells at the onset of obesity. Nat. Cell Biol 17, 376–385. 10.1038/ncb3122. [PubMed: 25730471]

16. Wang QA, Tao C, Gupta RK, and Scherer PE (2013). Tracking adipogenesis during white adipose tissue development, expansion and regeneration. Nat. Med 19, 1338–1344. 10.1038/nm.3324. [PubMed: 23995282]

17. Berry R, and Rodeheffer MS (2013). Characterization of the adipocyte cellular lineage in vivo. Nat. Cell Biol 15, 302–308. 10.1038/ncb2696. [PubMed: 23434825]

18. Jeffery E, Wing A, Holtrup B, Sebo Z, Kaplan JL, Saavedra-Peña R, Church CD, Colman L, Berry R, and Rodeheffer MS (2016). The Adipose Tissue Microenvironment Regulates Depot-Specific Adipogenesis in Obesity. Cell Metab. 24, 142–150. 10.1016/j.cmet.2016.05.012. [PubMed: 27320063]

19. Cao H, Gerhold K, Mayers JR, Wiest MM, Watkins SM, and Hotamisligil GS (2008). Identification of a lipokine, a lipid hormone linking adipose tissue to systemic metabolism. Cell 134, 933–944. 10.1016/j.cell.2008.07.048. [PubMed: 18805087]

20. Pisani DF, Ghandour RA, Beranger GE, Le Faouder P, Chambard JC, Giroud M, Vegiopoulos A, Djedaini M, Bertrand-Michel J, Tauc M, et al. (2014). The omega 6-fatty acid, arachidonic acid, regulates the conversion of white to brite adipocyte through a prostaglandin/calcium mediated pathway. Mol. Metab 3, 834–847. 10.1016/j.molmet.2014.09.003. [PubMed: 25506549]

21. Vellers HL, Letsinger AC, Walker NR, Granados JZ, and Lightfoot JT (2017). High Fat High Sugar Diet Reduces Voluntary Wheel Running in Mice Independent of Sex Hormone Involvement. Front. Physiol 8, 628. 10.3389/fphys.2017.00628. [PubMed: 28890701]

22. Licholai JA, Nguyen KP, Fobbs WC, Schuster CJ, Ali MA, and Kravitz AV (2018). Why Do Mice Overeat High-Fat Diets? How High-Fat Diet Alters the Regulation of Daily Caloric Intake in Mice. Obesity 26, 1026–1033. 10.1002/oby.22195. [PubMed: 29707908]

23. Hatori M, Vollmers C, Zarrinpar A, Ditacchio L, Bushong EA, Gill S, Leblanc M, Chaix A, Joens M, Fitzpatrick JAJ, et al. (2013). Time-Restricted Feeding Without Reducing Caloric Intake Prevents Metabolic Diseases in Mice Fed a High-Fat Diet. Diabetes 62, A526.

24. Nightingale Health for Research (n. n). Biomarker-wide association plots. https://research.nightingalehealth.com/atlas/biomarker-wide-association-plots.

25. Gagnon A, and Sorisky A (1998). The effect of glucose concentration on insulin-induced 3T3-L1 adipose cell differentiation. Obes. Res 6, 157–163. 10.1002/j.1550-8528.1998.tb00330.x. [PubMed: 9545023]

26. Cen J, Sargsyan E, and Bergsten P (2016). Fatty acids stimulate insulin secretion from human pancreatic islets at fasting glucose concentrations via mitochondria-dependent and -independent mechanisms. Nutr. Metab 13, 59. 10.1186/s12986-016-0119-5.

27. Stein DT, Stevenson BE, Chester MW, Basit M, Daniels MB, Turley SD, and McGarry JD (1997). The insulinotropic potency of fatty acids is influenced profoundly by their chain length and degree of saturation. J. Clin. Investig 100, 398–403. 10.1172/JCI119546. [PubMed: 9218517]

28. Liu AX, Testa JR, Hamilton TC, Jove R, Nicosia SV, and Cheng JQ (1998). AKT2, a member of the protein kinase B family, is activated by growth factors, v-Ha-ras, and v-src through phosphatidylinositol 3-kinase in human ovarian epithelial cancer cells. Cancer Res. 58, 2973–2977. [PubMed: 9679957]

29. Mitsuuchi Y, Johnson SW, Moonblatt S, and Testa JR (1998). Translocation and activation of AKT2 in response to stimulation by insulin. J. Cell. Biochem 70, 433–441. [PubMed: 9712142]

30. Julkunen H, Cichońska A, Tiainen M, Koskela H, Nybo K, Mäkelä V, Nokso-Koivisto J, Kristiansson K, Perola M, Salomaa V, et al. (2023). Atlas of plasma NMR biomarkers for health and disease in 118,461 individuals from the UK Biobank. Nat. Commun 14, 604. 10.1038/s41467-023-36231-7. [PubMed: 36737450]

31. Zhang L, Liu Z, Zhang W, Wang J, Kang H, Jing J, Han L, and Gao A (2024). Gut microbiota-palmitoleic acid-interleukin-5 axis orchestrates benzene-induced hematopoietic toxicity. Gut Microbes 16, 2323227. 10.1080/19490976.2024.2323227. [PubMed: 38436067]

32. Rossmeisl M, Pavlisova J, Bardova K, Kalendova V, Buresova J, Kuda O, Kroupova P, Stankova B, Tvrzicka E, Fiserova E, et al. (2020). Increased plasma levels of palmitoleic acid may contribute

to beneficial effects of Krill oil on glucose homeostasis in dietary obese mice. Biochim. Biophys. Acta. Mol. Cell Biol. Lipids 1865, 158732. 10.1016/j.bbalip.2020.158732. [PubMed: 32371092]

33. Hilgendorf KI, Johnson CT, Mezger A, Rice SL, Norris AM, Demeter J, Greenleaf WJ, Reiter JF, Kopinke D, and Jackson PK (2019). Omega-3 Fatty Acids Activate Ciliary FFAR4 to Control Adipogenesis. Cell 179, 1289–1305.e21. 10.1016/j.cell.2019.11.005. [PubMed: 31761534]
34. Briscoe CP, Tadayyon M, Andrews JL, Benson WG, Chambers JK, Eilert MM, Ellis C, Elshourbagy NA, Goetz AS, Minnick DT, et al. (2003). The orphan G protein-coupled receptor GPR40 is activated by medium and long chain fatty acids. J. Biol. Chem 278, 11303–11311. 10.1074/jbc.M211495200. [PubMed: 12496284]
35. Hirasawa A, Tsumaya K, Awaji T, Katsuma S, Adachi T, Yamada M, Sugimoto Y, Miyazaki S, and Tsujimoto G (2005). Free fatty acids regulate gut incretin glucagon-like peptide-1 secretion through GPR120. Nat. Med 11, 90–94. 10.1038/nm1168. [PubMed: 15619630]
36. Bjursell M, Xu X, Admyre T, Böttcher G, Lundin S, Nilsson R, Stone VM, Morgan NG, Lam YY, Storlien LH, et al. (2014). The beneficial effects of n-3 polyunsaturated fatty acids on diet induced obesity and impaired glucose control do not require Gpr120. PLoS One 9, e114942. 10.1371/journal.pone.0114942. [PubMed: 25541716]
37. Latour MG, Alquier T, Oseid E, Tremblay C, Jetton TL, Luo J, Lin DCH, and Poitout V (2007). GPR40 is necessary but not sufficient for fatty acid stimulation of insulin secretion in vivo. Diabetes 56, 1087–1094. 10.2337/db06-1532. [PubMed: 17395749]
38. Kim KH, Lee GY, Kim JI, Ham M, Won Lee J, and Kim JB (2010). Inhibitory effect of LXR activation on cell proliferation and cell cycle progression through lipogenic activity. J. Lipid Res 51, 3425–3433. 10.1194/jlr.M007989. [PubMed: 20847297]
39. Matsushita K, Morello F, Zhang Z, Masuda T, Iwanaga S, Steffensen KR, Gustafsson JÅ, Pratt RE, and Dzau VJ (2016). Nuclear hormone receptor LXR alpha inhibits adipocyte differentiation of mesenchymal stem cells with Wnt/beta-catenin signaling. Lab. Invest 96, 230–238. 10.1038/labinvest.2015.141. [PubMed: 26595172]
40. Pawar A, Xu J, Jerks E, Mangelsdorf DJ, and Jump DB (2002). Fatty acid regulation of liver X receptors (LXR) and peroxisome proliferator-activated receptor alpha (PPARalpha) in HEK293 cells. J. Biol. Chem 277, 39243–39250. 10.1074/jbc.M206170200. [PubMed: 12161442]
41. Schultz JR, Tu H, Luk A, Repa JJ, Medina JC, Li L, Schwendner S, Wang S, Thoolen M, Mangelsdorf DJ, et al. (2000). Role of LXRs in control of lipogenesis. Genes Dev. 14, 2831–2838. 10.1101/gad.850400. [PubMed: 11090131]
42. Ntambi JM (1995). The regulation of stearoyl-CoA desaturase (SCD). Prog. Lipid Res 34, 139–150. 10.1016/0163-7827(94)00010-j. [PubMed: 7480063]
43. Torra IP, Ismaili N, Feig JE, Xu CF, Cavasotto C, Pancratov R, Rogatsky I, Neubert TA, Fisher EA, and Garabedian MJ (2008). Phosphorylation of liver x receptor alpha selectively regulates target gene expression in macrophages. Mol. Cell Biol 28, 2626–2636. 10.1128/Mcb.01575-07. [PubMed: 18250151]
44. Gage MC, Becares N, Louie R, Waddington KE, Zhang Y, Tittanegro TH, Rodriguez-Lorenzo S, Jathanna A, Pourcet B, Pello OM, et al. (2018). Disrupting LXRalpha phosphorylation promotes FoxM1 expression and modulates atherosclerosis by inducing macrophage proliferation. Proc. Natl. Acad. Sci. USA 115, E6556–E6565. 10.1073/pnas.1721245115. [PubMed: 29950315]
45. Willy PJ, Umesono K, Ong ES, Evans RM, Heyman RA, and Mangelsdorf DJ (1995). Lxr, a Nuclear Receptor That Defines a Distinct Retinoid Response Pathway. Gene Dev. 9, 1033–1045. 10.1101/gad.9.9.1033. [PubMed: 7744246]
46. Apfel R, Benbrook D, Lernhardt E, Ortiz MA, Salbert G, and Pfahl M (1994). A Novel Orphan Receptor-Specific for a Subset of Thyroid Hormone-Responsive Elements and Its Interaction with the Retinoid/Thyroid Hormone-Receptor Subfamily. Mol. Cell Biol 14, 7025–7035. 10.1128/Mcb.14.10.7025. [PubMed: 7935418]
47. Saavedra-Pena RD, Taylor N, Flannery C, and Rodeheffer MS (2023). Estradiol cycling drives female obesogenic adipocyte hyperplasia. Cell Rep. 42, 112390. 10.1016/j.celrep.2023.112390. [PubMed: 37053070]
48. Farmer SR (2006). Transcriptional control of adipocyte formation. Cell Metab. 4, 263–273. 10.1016/j.cmet.2006.07.001. [PubMed: 17011499]

49. Rosen ED, Hsu CH, Wang X, Sakai S, Freeman MW, Gonzalez FJ, and Spiegelman BM (2002). C/EBPalpha induces adipogenesis through PPARgamma: a unified pathway. Genes Dev. 16, 22–26. 10.1101/gad.948702. [PubMed: 11782441]
50. Cristancho AG, and Lazar MA (2011). Forming functional fat: a growing understanding of adipocyte differentiation. Nat. Rev. Mol. Cell Biol 12, 722–734. 10.1038/nrm3198. [PubMed: 21952300]
51. Venkateswaran A, Laffitte BA, Joseph SB, Mak PA, Wilpitz DC, Edwards PA, and Tontonoz P (2000). Control of cellular cholesterol efflux by the nuclear oxysterol receptor LXR alpha. Proc. Natl. Acad. Sci. USA 97, 12097–12102. 10.1073/pnas.200367697. [PubMed: 11035776]
52. Peet DJ, Turley SD, Ma W, Janowski BA, Lobaccaro JM, Hammer RE, and Mangelsdorf DJ (1998). Cholesterol and bile acid metabolism are impaired in mice lacking the nuclear oxysterol receptor LXR alpha. Cell 93, 693–704. 10.1016/s00928674(00)814324. [PubMed: 9630215]
53. Repa JJ, Liang G, Ou J, Bashmakov Y, Lobaccaro JM, Shimomura I, Shan B, Brown MS, Goldstein JL, and Mangelsdorf DJ (2000). Regulation of mouse sterol regulatory element-binding protein-1c gene (SREBP-1c) by oxysterol receptors, LXRalpha and LXRbeta. Genes Dev. 14, 2819–2830. 10.1101/gad.844900. [PubMed: 11090130]
54. Belorusova AY, Evertsson E, Hovdal D, Sandmark J, Bratt E, Maxvall I, Schulman IG, Åkerblad P, and Lindstedt EL (2019). Structural analysis identifies an escape route from the adverse lipogenic effects of liver X receptor ligands. Commun. Biol 2, 431. 10.1038/s42003019-06750. [PubMed: 31799433]
55. Dang H, Liu Y, Pang W, Li C, Wang N, Shyy JYJ, and Zhu Y (2009). Suppression of 2,3-oxidosqualene cyclase by high fat diet contributes to liver X receptor-alpha-mediated improvement of hepatic lipid profile. J. Biol. Chem 284, 6218–6226. 10.1074/jbc.M803702200. [PubMed: 19119143]
56. Komati R, Spadoni D, Zheng S, Sridhar J, Riley KE, and Wang G (2017). Ligands of Therapeutic Utility for the Liver X Receptors. Molecules 22, 88. 10.3390/molecules22010088. [PubMed: 28067791]
57. Becares N, Gage MC, Voisin M, Shrestha E, Martin-Gutierrez L, Liang N, Louie R, Pourcet B, Pello OM, Luong TV, et al. (2019). Impaired LXR alpha Phosphorylation Attenuates Progression of Fatty Liver Disease. Cell Rep. 26, 984–995.e6. 10.1016/j.cel-rep.2018.12.094. [PubMed: 30673619]
58. Seo JB, Moon HM, Kim WS, Lee YS, Jeong HW, Yoo EJ, Ham J, Kang H, Park MG, Steffensen KR, et al. (2004). Activated liver X receptors stimulate adipocyte differentiation through induction of peroxisome proliferator-activated receptor gamma expression. Mol. Cell Biol 24, 3430–3444. 10.1128/Mcb.24.8.34303444.2004. [PubMed: 15060163]
59. Laurencikiene J, and Rydén M (2012). Liver X receptors and fat cell metabolism. Int. J. Obes 36, 1494–1502. 10.1038/ijo.2012.21.
60. Ross SE, Erickson RL, Gerin I, DeRose PM, Bajnok L, Longo KA, Misek DE, Kuick R, Hanash SM, Atkins KB, et al. (2002). Microarray analyses during adipogenesis: understanding the effects of Wnt signaling on adipogenesis and the roles of liver X receptor alpha in adipocyte metabolism. Mol. Cell Biol 22, 5989–5999. 10.1128/MCB.22.16.59895999.2002. [PubMed: 12138207]
61. Ou J, Tu H, Shan B, Luk A, DeBose-Boyd RA, Bashmakov Y, Goldstein JL, and Brown MS (2001). Unsaturated fatty acids inhibit transcription of the sterol regulatory element-binding protein-1c (SREBP-1c) gene by antagonizing ligand-dependent activation of the LXR. Proc. Natl. Acad. Sci. USA 98, 6027–6032. 10.1073/pnas.111138698. [PubMed: 11371634]
62. Zhao Z, Xu D, Li S, He B, Huang Y, Xu M, Ren S, Li S, Wang H, and Xie W (2016). Activation of Liver X Receptor Attenuates Oleic Acid-Induced Acute Respiratory Distress Syndrome. Am. J. Pathol 186, 2614–2622. 10.1016/j.ajpath.2016.06.018. [PubMed: 27520356]
63. Ducheix S, Montagner A, Polizzi A, Lasserre F, Régnier M, Marmugi A, Benhamed F, Bertrand-Michel J, Mselli-Lakhal L, Loiseau N, et al. (2017). Dietary oleic acid regulates hepatic lipogenesis through a liver X receptor-dependent signaling. PLoS One 12, e0181393. 10.1371/journal.pone.0181393. [PubMed: 28732092]
64. Poungvarin N, Chang B, Imamura M, Chen J, Moolsuwan K, Sae-Lee C, Li W, and Chan L (2015). Genome-Wide Analysis of ChREBP Binding Sites on Male Mouse Liver and White Adipose Chromatin. Endocrinology 156, 1982–1994. 10.1210/en.20141666. [PubMed: 25751637]

65. Meroni M, De Caro E, Chiappori F, Longo M, Paolini E, Mosca E, Merelli I, Lombardi R, Badiali S, Maggioni M, et al. (2024). Hepatic and adipose tissue transcriptome analysis highlights a commonly deregulated autophagic pathway in severe MASLD. Obesity 32, 923–937. 10.1002/oby.23996. [PubMed: 38439203]
66. Chu K, Miyazaki M, Man WC, and Ntambi JM (2006). Stearoyl-co-enzyme A desaturase 1 deficiency protects against hypertriglyceridemia and increases plasma high-density lipoprotein cholesterol induced by liver X receptor activation. Mol. Cell Biol 26, 6786–6798. 10.1128/MCB.0007706. [PubMed: 16943421]
67. Yamamoto T, Shimano H, Inoue N, Nakagawa Y, Matsuzaka T, Takahashi A, Yahagi N, Sone H, Suzuki H, Toyoshima H, and Yamada N (2007). Protein kinase A suppresses sterol regulatory element-binding protein-1C expression via phosphorylation of liver X receptor in the liver. J. Biol. Chem 282, 11687–11695. 10.1074/jbc.M611911200. [PubMed: 17296605]
68. Delvecchio CJ, and Capone JP (2008). Protein kinase C alpha modulates liver X receptor alpha transactivation. J. Endocrinol 197, 121–130. 10.1677/JOE-070525. [PubMed: 18372238]
69. Abbott SK, Else PL, Atkins TA, and Hulbert AJ (2012). Fatty acid composition of membrane bilayers: importance of diet polyunsaturated fat balance. Biochim. Biophys. Acta 1818, 1309–1317. 10.1016/j.bbamem.2012.01.011. [PubMed: 22285120]
70. Rong X, Albert CJ, Hong C, Duerr MA, Chamberlain BT, Tarling EJ, Ito A, Gao J, Wang B, Edwards PA, et al. (2013). LXRs regulate ER stress and inflammation through dynamic modulation of membrane phospholipid composition. Cell Metab. 18, 685–697. 10.1016/j.cmet.2013.10.002. [PubMed: 24206663]
71. Teres S, Llado V, Higuera M, Barcelo-Coblijn G, Martin ML, Noguera-Salva MA, Marcilla-Etxenike A, Garcia-Verdugo JM, Soriano-Navarro M, Saus C, et al. (2012). 2-Hydroxyoleate, a nontoxic membrane binding anticancer drug, induces glioma cell differentiation and autophagy. Proc. Natl. Acad. Sci. USA 109, 8489–8494. 10.1073/pnas.1118349109. [PubMed: 22586083]
72. Wang B, Rong X, Palladino END, Wang J, Fogelman AM, Martín MG, Alrefai WA, Ford DA, and Tontonoz P (2018). Phospholipid Remodeling and Cholesterol Availability Regulate Intestinal Stemness and Tumorigenesis. Cell Stem Cell 22, 206–220.e4. 10.1016/j.stem.2017.12.017. [PubMed: 29395055]
73. Wang F, Vihma V, Soronen J, Turpeinen U, Hämäläinen E, Savolainen-Peltonen H, Mikkola TS, Naukkarinen J, Pietiläinen KH, Jauhiainen M, et al. (2013). 17beta-Estradiol and estradiol fatty acyl esters and estrogen-converting enzyme expression in adipose tissue in obese men and women. J. Clin. Endocrinol. Metab 98, 4923–4931. 10.1210/jc.20132605. [PubMed: 24081738]
74. Mair KM, Harvey KY, Henry AD, Hillyard DZ, Nilsen M, and MacLean MR (2019). Obesity alters oestrogen metabolism and contributes to pulmonary arterial hypertension. Eur. Respir. J 53, 1801524. 10.1183/13993003.015242018. [PubMed: 30923189]
75. Pettersson AML, Stenson BM, Lorente-Cebrián S, Andersson DP, Mejhert N, Krätzel J, Aström G, Dahlman I, Chibalin AV, Arner P, and Laurencikiene J (2013). LXR is a negative regulator of glucose uptake in human adipocytes. Diabetologia 56, 2044–2054. 10.1007/s00125013-29545. [PubMed: 23765184]
76. Pommier AJC, Alves G, Viennois E, Bernard S, Communal Y, Sion B, Marceau G, Damon C, Mouzat K, Caira F, et al. (2010). Liver X Receptor activation downregulates AKT survival signaling in lipid rafts and induces apoptosis of prostate cancer cells. Oncogene 29, 2712–2723. 10.1038/onc.2010.30. [PubMed: 20190811]
77. Vedin LL, Lewandowski SA, Parini P, Gustafsson JA, and Steffensen KR (2009). The oxysterol receptor LXR inhibits proliferation of human breast cancer cells. Carcinogenesis 30, 575–579. 10.1093/carcin/bgp029. [PubMed: 19168586]
78. Gong H, Guo P, Zhai Y, Zhou J, Uppal H, Jarzynka MJ, Song WC, Cheng SY, and Xie W (2007). Estrogen deprivation and inhibition of breast cancer growth in vivo through activation of the orphan nuclear receptor liver X receptor. Mol. Endocrinol 21, 1781–1790. 10.1210/me.20070187. [PubMed: 17536009]
79. Sun M, Paciga JE, Feldman RI, Yuan Z, Coppola D, Lu YY, Shelley SA, Nicosia SV, and Cheng JQ (2001). Phosphatidylinositol-3-OH Kinase (PI3K)/AKT2, activated in breast cancer, regulates and is induced by estrogen receptor alpha (ERalpha) via interaction between ERalpha and PI3K. Cancer Res. 61, 5985–5991. [PubMed: 11507039]

80. Kim JY, van de Wall E, Laplante M, Azzara A, Trujillo ME, Hofmann SM, Schraw T, Durand JL, Li H, Li G, et al. (2007). Obesity-associated improvements in metabolic profile through expansion of adipose tissue. J. Clin. Investig 117, 2621–2637. 10.1172/Jci31021. [PubMed: 17717599]
81. Jang H, Kim M, Lee S, Kim J, Woo DC, Kim KW, Song K, and Lee I (2016). Adipose tissue hyperplasia with enhanced adipocyte-derived stem cell activity in Tc1(C8orf4)-deleted mice. Sci. Rep 6, 35884. 10.1038/srep35884. [PubMed: 27775060]
82. Doege H, Grimm D, Falcon A, Tsang B, Storm TA, Xu H, Ortegon AM, Kazantzis M, Kay MA, and Stahl A (2008). Silencing of hepatic fatty acid transporter protein 5 in vivo reverses diet-induced non-alcoholic fatty liver disease and improves hyperglycemia. J. Biol. Chem 283, 22186–22192. 10.1074/jbc.M803510200. [PubMed: 18524776]
83. Orellana-Gavalda JM, Herrero L, Malandrino MI, Paneda A, Sol Rodriguez-Pena M, Petry H, Asins G, Van Deventer S, Hegardt FG, and Serra D (2011). Molecular therapy for obesity and diabetes based on a long-term increase in hepatic fatty-acid oxidation. Hepatology 53, 821–832. 10.1002/hep.24140. [PubMed: 21319201]
84. Kim JY, Hickner RC, Cortright RL, Dohm GL, and Houmard JA (2000). Lipid oxidation is reduced in obese human skeletal muscle. Am. J. Physiol. Endocrinol. Metab 279, E1039–E1044. 10.1152/ajpendo.2000.279.5.E1039. [PubMed: 11052958]
85. Vessby B, Uusitupa M, Hermansen K, Riccardi G, Rivellese AA, Tapsell LC, Nälsén C, Berglund L, Louheranta A, Rasmussen BM, et al. (2001). Substituting dietary saturated for monounsaturated fat impairs insulin sensitivity in healthy men and women: The KANWU Study. Diabetologia 44, 312–319. 10.1007/s001250051620. [PubMed: 11317662]
86. Perdomo L, Beneit N, Otero YF, Escribano Ó, Díaz-Castroverde S, Gómez-Hernández A, and Benito M (2015). Protective role of oleic acid against cardiovascular insulin resistance and in the early and late cellular atherosclerotic process. Cardiovasc. Diabetol 14, 75. 10.1186/s12933015-02379. [PubMed: 26055507]
87. Moon JH, Lee JY, Kang SB, Park JS, Lee BW, Kang ES, Ahn CW, Lee HC, and Cha BS (2010). Dietary Monounsaturated Fatty Acids but not Saturated Fatty Acids Preserve the Insulin Signaling Pathway via IRS-1/PI3K in Rat Skeletal Muscle. Lipids 45, 1109–1116. 10.1007/s11745010-34753. [PubMed: 20960069]
88. Delgado GE, Kramer BK, Lorkowski S, Marz W, von Schacky C, and Kleber ME (2017). Individual omega-9 monounsaturated fatty acids and mortality-The Ludwigshafen Risk and Cardiovascular Health Study. J Clin Lipidol 11, 126–135.e125. 10.1016/j.jacl.2016.10.015. [PubMed: 28391879]
89. Steffen BT, Duprez D, Szklo M, Guan W, and Tsai MY (2018). Circulating oleic acid levels are related to greater risks of cardiovascular events and all-cause mortality: The Multi-Ethnic Study of Atherosclerosis. J. Clin. Lipidol 12, 1404–1412. 10.1016/j.jacl.2018.08.004. [PubMed: 30201531]
90. Baer DJ, Henderson T, and Gebauer SK (2021). Consumption of High-Oleic Soybean Oil Improves Lipid and Lipoprotein Profile in Humans Compared to a Palm Oil Blend: A Randomized Controlled Trial. Lipids 56, 313–325. 10.1002/lipd.12298. [PubMed: 33596340]
91. Xia M, Zhong Y, Peng Y, and Qian C (2022). Olive oil consumption and risk of cardiovascular disease and all-cause mortality: A meta-analysis of prospective cohort studies. Front. Nutr 9, 1041203. 10.3389/fnut.2022.1041203. [PubMed: 36330142]
92. Blasbalg TL, Hibbeln JR, Ramsden CE, Majchrzak SF, and Rawlings RR (2011). Changes in consumption of omega-3 and omega-6 fatty acids in the United States during the 20th century. Am. J. Clin. Nutr 93, 950–962. 10.3945/ajcn.110.006643. [PubMed: 21367944]
93. Shields DS (2010). Prospecting for oil. Gastronomica 10, 25–34. 10.1525/gfc.2010.10.4.25. [PubMed: 21568041]
94. Garsetti M, Balentine DA, Zock PL, Blom WAM, and Wanders AJ (2016). Fat composition of vegetable oil spreads and margarines in the USA in 2013: a national marketplace analysis. Int. J. Food Sci. Nutr 67, 372–382. 10.3109/09637486.2016.1161012. [PubMed: 27046021]
95. Huth PJ, Fulgoni VL 3rd, and Larson BT (2015). A systematic review of high-oleic vegetable oil substitutions for other fats and oils on cardiovascular disease risk factors: implications for novel high-oleic soybean oils. Adv. Nutr 6, 674–693. 10.3945/an.115.008979. [PubMed: 26567193]

96. Wallis JG, Bengtsson JD, and Browse J (2022). Molecular Approaches Reduce Saturates and Eliminate trans Fats in Food Oils. Front. Plant Sci 13, 908608. 10.3389/fpls.2022.908608. [PubMed: 35720592]

97. US FDA (2018). FDA Completes Review of Qualified Health Claim Petition for Oleic Acid and the Risk of Coronary Heart Disease. https://www.fda.gov/food/hfp-constituent-updates/fda-completes-review-qualified-health-claim-petition-oleic-acid-and-risk-coronary-heart-disease

98. Bowen KJ, Kris-Etherton PM, West SG, Fleming JA, Connelly PW, Lamarche B, Couture P, Jenkins DJA, Taylor CG, Zahradka P, et al. (2019). Diets Enriched with Conventional or High-Oleic Acid Canola Oils Lower Atherogenic Lipids and Lipoproteins Compared to a Diet with a Western Fatty Acid Profile in Adults with Central Adiposity. J. Nutr 149, 471–478. 10.1093/jn/nxy307. [PubMed: 30773586]

99. Saavedra-Pena RDM, Taylor N, and Rodeheffer MS (2022). Insights of the role of estrogen in obesity from two models of ERalpha deletion. J. Mol. Endocrinol 68, 179–194. 10.1530/JME-210260. [PubMed: 35244608]

100. Voisin M, Shrestha E, Rollet C, Nikain CA, Josefs T, Mahé M, Barrett TJ, Chang HR, Ruoff R, Schneider JA, et al. (2021). Inhibiting LXRalpha phosphorylation in hematopoietic cells reduces inflammation and attenuates atherosclerosis and obesity in mice. Commun. Biol 4, 420. 10.1038/s42003021-019255. [PubMed: 33772096]

101. Carpenter AE, Jones TR, Lamprecht MR, Clarke C, Kang IH, Friman O, Guertin DA, Chang JH, Lindquist RA, Moffat J, et al. (2006). CellProfiler: image analysis software for identifying and quantifying cell phenotypes. Genome Biol. 7, R100. 10.1186/gb-20067-10-r100. [PubMed: 17076895]

102. Trapnell C, Pachter L, and Salzberg SL (2009). TopHat: discovering splice junctions with RNA-Seq. Bioinformatics 25, 1105–1111. 10.1093/bioinformatics/btp120. [PubMed: 19289445]

103. Anders S, Pyl PT, and Huber W (2015). HTSeq–a Python framework to work with high-throughput sequencing data. Bioinformatics 31, 166–169. 10.1093/bioinformatics/btu638. [PubMed: 25260700]

104. Love MI, Huber W, and Anders S (2014). Moderated estimation of fold change and dispersion for RNA-seq data with DESeq2. Genome Biol. 15, 550. 10.1186/s13059014-05508. [PubMed: 25516281]

105. Berry R, Church CD, Gericke MT, Jeffery E, Colman L, and Rodeheffer MS (2014). Imaging of adipose tissue. Methods Enzymol. 537, 47–73. 10.1016/B9780-12411619-1.000045. [PubMed: 24480341]

106. Rodeheffer MS, Birsoy K, and Friedman JM (2008). Identification of White Adipocyte Progenitor Cells In Vivo. Cell 135, 240–249. 10.1016/j.cell.2008.09.036. [PubMed: 18835024]

107. Speakman JR, de Jong JMA, Sinha S, Westerterp KR, Yamada Y, Sagayama H, Ainslie PN, Anderson LJ, Arab L, Bedu-Addo K, et al. (2023). Total daily energy expenditure has declined over the past three decades due to declining basal expenditure, not reduced activity expenditure. Nat. Metab 5, 579–588. 10.1038/s42255023-007822. [PubMed: 37100994]

108. Varshney R, Das S, Trahan GD, Farriester JW, Mullen GP, Kyere-Davies G, Presby DM, Houck JA, Webb PG, Dzieciatkowska M, et al. (2023). Neonatal intake of Omega-3 fatty acids enhances lipid oxidation in adipocyte precursors. iScience 26, 105750. 10.1016/j.isci.2022.105750. [PubMed: 36590177]

Highlights

- Fat composition of HFD modulates adipose hyperplasia
- Dietary OA is the sole fatty acid that drives adipogenesis at physiological levels
- OA-induced adipogenesis depends on AKT2 signaling and decreased LXR activity
- LXRα phosphorylation in APCs inhibits HFD-induced proliferation

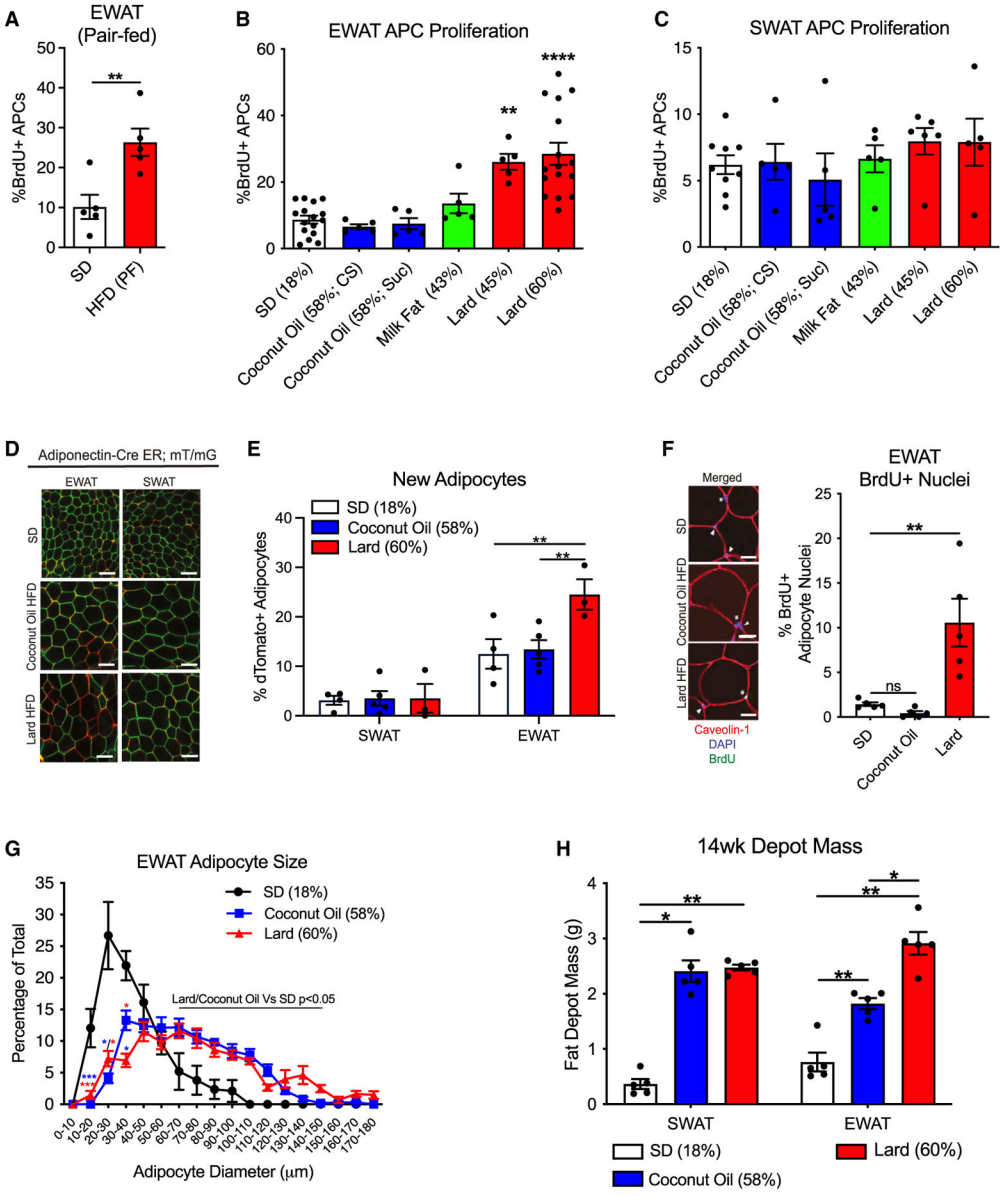

Figure 1. Dietary fat composition modulates obesogenic adipogenesis

(A) EWAT APC proliferation after 1 week of SD consumption or HFD (60% kcal lard fat) pair-fed to SD ($n = 5$).

(B and C) EWAT (B) and SWAT (C) APC proliferation after 1 week of diet consumption ($n = 5–16$).

(D and E) Representative images (D) and quantification (E) of traced adipocytes after tamoxifen treatment and 8-week diet consumption. Scale bar: 100 μm ($n = 3–5$).

(F) Representative images and quantification of adipocyte nuclei after diet and 1-week BrdU pulse and 7-week chase. Asterisks: adipocyte nuclei; arrows: nonadipocyte nuclei. Scale bar: 25 μm ($n = 5$).

(G and H) Distribution of EWAT adipocyte size (G) and fat depot mass (H) after 20-week diet consumption ($n = 5–8$).

See also Figure S1. Data are represented as mean ± SEM. Statistical significance was identified by t test (A), one-way ANOVA multiple comparisons to SD (B, C, F, and G), or two-way ANOVA multiple comparisons (E and H). Coconut diet containing sucrose was used for (C)–(I). *$p < 0.05$, **$p < 0.01$, and ****$p < 0.0001$.

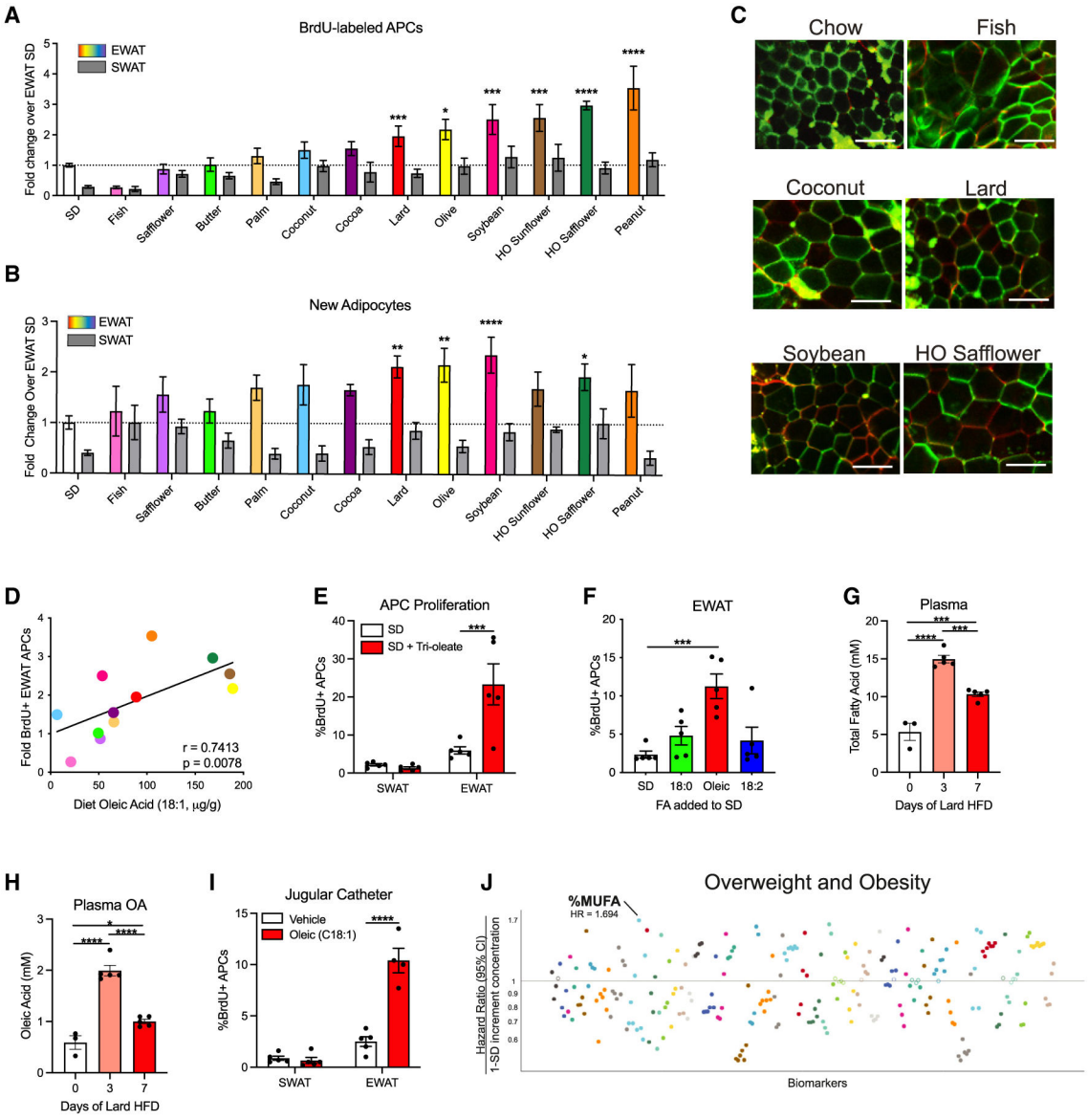

Figure 2. Oleic acid is a diet-derived driver of APC proliferation

(A) Fold change of EWAT and SWAT APC proliferation normalized to EWAT SD. Mice were fed diets for 1 week with BrdU water (n = 5–20).

(B and C) Fold change of new adipocytes in EWAT and SWAT normalized to EWAT SD (B) and representative images (C). AdiER mice were treated with tamoxifen and then given a diet for 8 weeks. Scale bar: 100 μm (n = 3–17).

(D) Correlation between dietary OA content and fold change diet average of EWAT APC proliferation over SD (Spearman's correlation).

(E) APC proliferation of mice given either SD or SD with 45% kcal tri-oleate for 7 days (n = 5).

(F) EWAT APC proliferation after 5 days consuming SD or SD with purified fatty acids (45% kcal) (n = 5).

(G and H) Total plasma fatty acid (G) and plasma OA (H) after consuming HFD (60% lard-based) ($n = 3–5$).

(I) APC proliferation after 5-day jugular infusion of BSA vehicle or OA (20 mM) ($n = 4–5$).

(J) Hazard ratios of 249 plasma metabolic biomarkers for obesity and overweight status from the UK Biobank. Solid dots indicate significant associations ($p < 0.000005$).[24] The data point for percent MUFA of total fatty acids in plasma is indicated.

See also Figure S1. Data are represented as mean ± SEM or mean by diet for correlation plots. Statistical significance was identified by one-way ANOVA multiple comparisons to SD (A, B, and H), one-way ANOVA (E and F), or two-way ANOVA multiple comparisons (G and I). *$p < 0.05$, **$p < 0.01$, ***$p < 0.001$, and ****$p < 0.0001$.

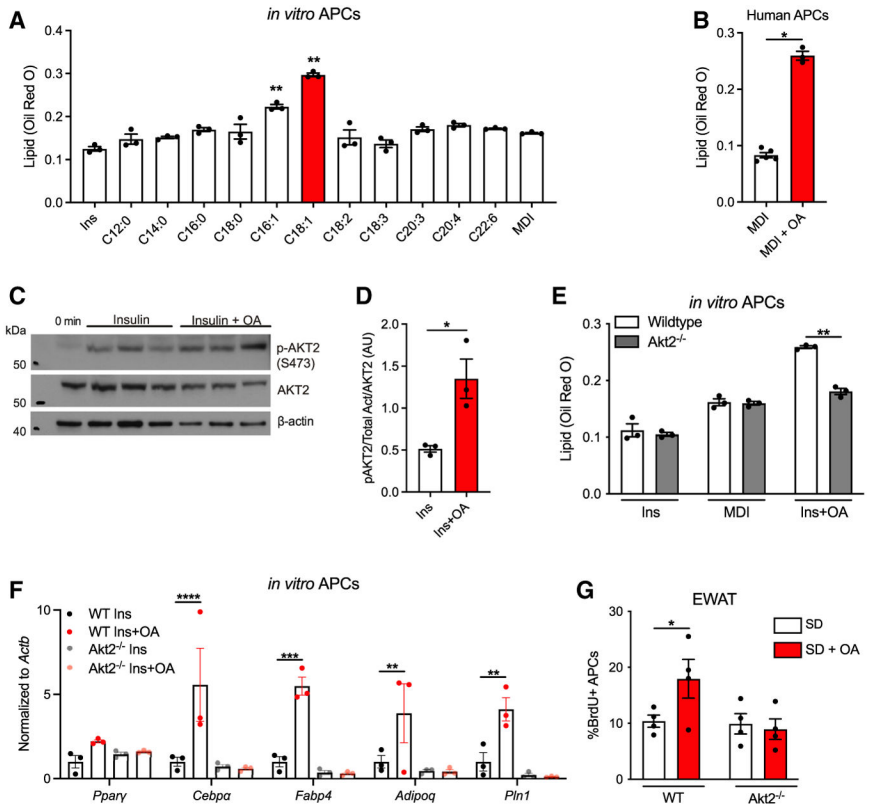

Figure 3. Oleic-acid-driven adipogenesis requires AKT2 signaling

(A) Lipid accumulation measured by oil red O extraction of primary APCs differentiated for 7 days with insulin, MDI, or insulin and 100 μM fatty acid ($n = 3$).

(B) Lipid accumulation measured by oil red O extraction in primary human APCs differentiated for 7 days with MDI or MDI and OA ($n = 3–5$).

(C and D) Western blot (C) and quantification (D) for pAKT2(Ser473), AKT2, and β-actin in primary APCs after insulin or insulin and OA for 3 h ($n = 3$).

(E) Lipid accumulation in WT or *Akt2*$^{-/-}$ APCs after 7 days of insulin, MDI, or insulin and OA ($n = 3$).

(F) qPCR of primary APCs from WT or *Akt2*$^{-/-}$ mice after 7 days of differentiation with insulin or insulin and OA ($n = 3$).

(G) Proliferation of EWAT APCs from WT or *AKT2*$^{-/-}$ mice fed HFD (60% lard based) for 7 days with BrdU ($n = 4$).

See also Figure S2. Cells were treated with 100 μM OA. Data are represented as mean ± SEM. Statistical significance was identified by one-way ANOVA multiple comparisons to insulin (A) or MDI (B), t test (B and C), or two-way ANOVA multiple comparisons (E–G). *$p < 0.05$, **$p < 0.01$, ***$p < 0.001$, and ****$p < 0.0001$.

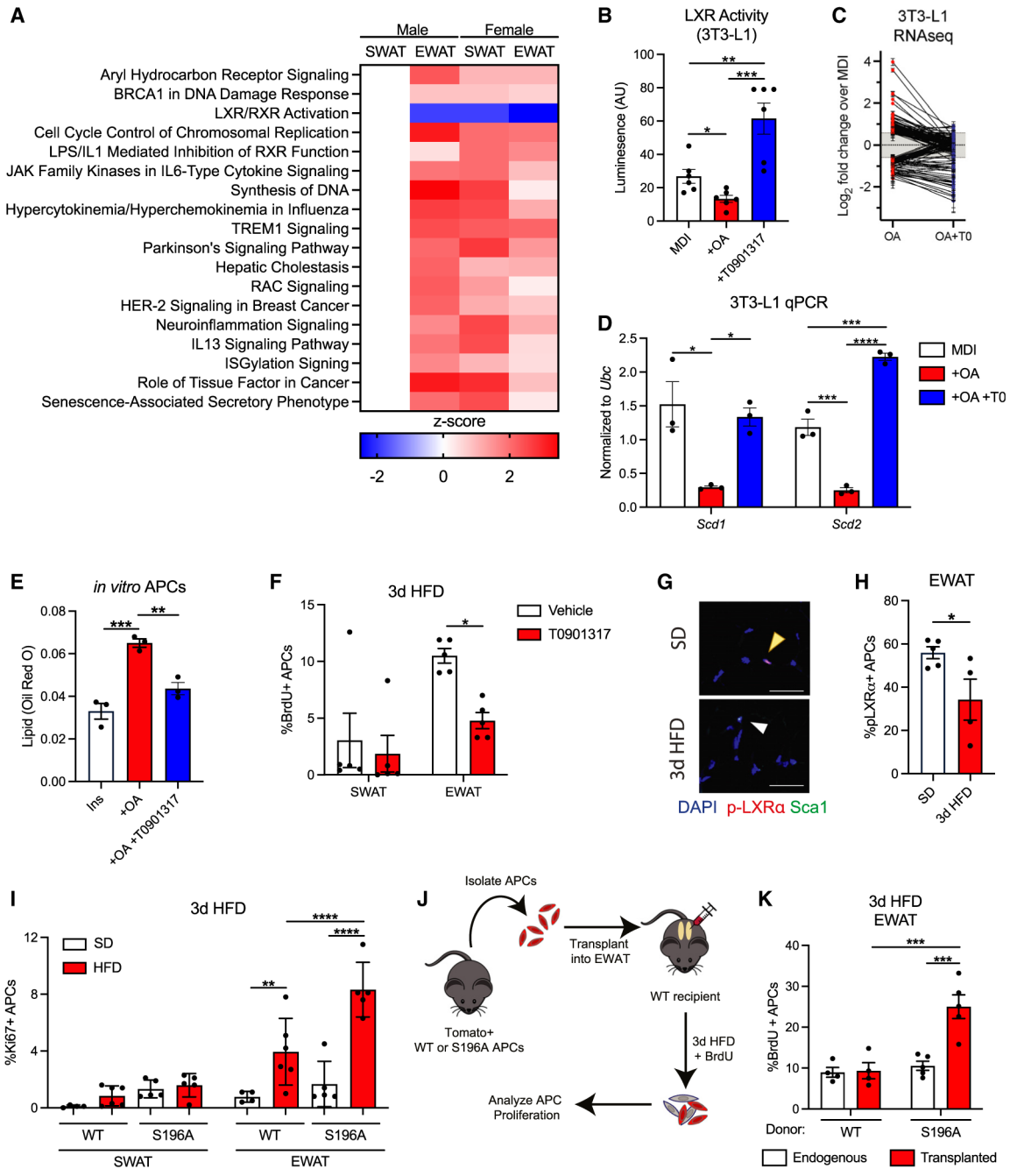

Figure 4. LXR signaling and phosphorylation inhibit diet-driven APC proliferation

(A) Heatmap of top pathway *Z* scores from RNA-seq of APCs from mice fed HFD (60% lard based) for 3 days. Pathways were selected as differentially regulated in male EWAT and female SWAT and EWAT but not male SWAT ($n = 3–5$).

(B) LXR activity quantified by a luciferase reporter assay in 3T3-L1 cells after 24 h treatment with MDI, MDI with OA, or MDI with T0901317 ($n = 6$).

(C) Log fold change of differentially expressed genes from 3T3-L1 cells after 24 h treatment with MDI supplemented with OA or with OA and T0901317.

(D) Gene expression of 3T3-L1 cells differentiated for 48 h with MDI, MDI with OA, or MDI with OA and T0 ($n = 3$).
(E) Lipid accumulation in primary APCs differentiated with insulin, insulin and OA, or insulin, OA, and T0901317 for 48 h ($n = 3$).
(F) Proliferation of APCs from mice treated with vehicle or T0901317 and fed HFD (60% lard based) for 3 days ($n = 5$).
(G and H) Representative images (G) and quantification (H) of pLXRα+ APCs (Sca1+) in EWAT of mice fed 60% HFD for 3 days. Scale bar: 25 μm($n = 4–5$).
(I) Percentage of proliferative APCs in SWAT and EWAT of WT or S196A mice fed HFD for 3 days ($n = 5–6$).
(J) Schematic of transplant experiment.
(K) Percentage of proliferative endogenous or transplanted APCs in EWAT of mice fed 60% HFD and treated with BrdU for 3 days ($n = 4$).
See also Figure S3. Cells were treated with 100 μM OA. Data are represented as mean ± SEM. Statistical significance as identified by t test (C, E, and H) or two-way ANOVA multiple comparisons (F, I, and K). *$p < 0.05$, **$p < 0.01$, ***$p < 0.001$, and ****$p < 0.0001$.

Table 1.

Correlation of fatty acids in diet and APC proliferation (averaged by diet)

Fatty acid	No. of pairs	*p* value	Spearman R
8:0	1	N/A	N/A
10:0	1	N/A	N/A
12:0	1	N/A	N/A
14:0	9	0.3853	−0.3333
14:1 *	8 *	0.0046 *	−0.9048 *
16:0	12	0.1845	−0.4126
16:1n-7	11	0.1928	−0.4273
16:2	6	0.4944	−0.3479
18:0	12	0.5731	−0.1818
18:1n-9 (oleic)[a]	12 *	0.0078 *	0.7413 *
18:2	12	0.2097	0.3916
18:3n-6	12	0.6832	−0.1329
18:3n-3	12	0.097	−0.5064
20:0	4	0.3333	0.8
20:1	5	0.95	0.1
20:2	7	0.8397	0.1071
20:3n-6	9	0.1352	−0.5439
20:3n-3	3	>0.9999	−0.5
20:4	8	0.206	−0.5123
20:5	11	0.3893	−0.287
22:1	12	0.5431	0.1958
22:4n-6	7	0.4444	−0.3571
22:5n-3	7	0.4563	−0.3424
22:6	4	0.3333	−0.8

[a]* Significant correlation between fatty acid in diet and APC proliferation.

KEY RESOURCES TABLE

REAGENT or RESOURCE	SOURCE	IDENTIFIER
Antibodies		
Rat anti-BrdU, 1:300	Abcam	6326, RRID:AB_305426
Rabbit Caveolin-1, 1:400	Cell Signaling Technology	3238, RRID:AB_2072166
Anti-rabbit Rhodamine-X-Red, 1:250	Jackson ImmunoResearch	111-295-144, RRID:AB_2338028
Anti-rat Alexa Fluor 488, 1:250	Jackson ImmunoResearch	112-545-167, RRID:AB_2338362
CD45 APC-eFluor780, 1:1000 for sorting, 1:500 for BrdU analysis	Thermo Fisher Scientific	47-0451-80, RRID:AB_1548790
CD31 PE-Cy7, 1:500	Thermo Fisher Scientific	25-0311-82, RRID:AB_2716949
CD29 Alexa Fluor 700, 1:400	BioLegend	102218, RRID:AB_2716949
CD34 Alexa Fluor 647, 1:400	Biolegend	119314, RRID:AB_604089
Sca1 Pacific Blue, 1:400	BD Biosciences	560653, RRID:AB1727553
CD24 PerCP-Cynanine 5.5, 1:250	eBioscience	45-0242-80, RRID:AB_1210702
Sca1 V500, 1:500	BD Horizon	561228, RRID:AB_10584334
CD34 Brilliant Violet 421, 1:400	BioLegend	119321, RRID:AB_10900980
Ki67 FITC, 1:50	Thermo Fisher Scientific	11-5698-80, RRID:AB_11151689
Rat Sca1, 1:50	BioLegend	122501, RRID:AB_756186
Rabbit *p*-LXRα, 1:50	Torra et al.[43]	https://doi.org/10.1128/MCB.01575-07
Anti-rat Alexa Fluor 647, 1:800	Jackson ImmunoResearch	112-605,003, RRID: AB_2338393
GP38 PE, 1:500	Biolegend	337003, RRID:AB_1595554
Rabbit Akt2, 1:1000	Cell Signaling	3063, RRID:AB_2225186
Rabbit phospho-Akt2, 1:500	Cell Signaling	8599, RRID:AB_2630347
Anti-rabbit HRP, 1:10,000	Jackson ImmunoResearch	211-032-171, RRID:AB_2339149
Phospho-AKT (S473) PE, 1:100	Cell Signaling	5315, RRID:AB_10694850
Phospho-AKT (T308) PE, 1:100	Cell Signaling	9088, RRID:AB_10891441
Chemicals, peptides, and recombinant proteins		
Tri-oleate	Millipore Sigma	T7140
Oleic acid (18:1)	Sigma	O1008
Stearic acid (18:0)	Cayman Chemical	10011298
Linoleic acid (18:2)	Cayman Chemical	90150
Lauric acid (12:0)	Cayman Chemical	10006626
Myristic acid (14:0)	Cayman Chemical	13351
Palmitic acid (16:0)	Cayman Chemical	10006627
Palmitoleic acid (16:1)	Cayman Chemical	10009871
Linolenic acid (18:3)	Cayman Chemical	90210
Dihomo-γ-linolenic acid (20:3)	Cayman Chemical	90230
Arachidonic acid (20:4)	Cayman Chemical	90010
Docosahexaenoic acid (22:6)	Cayman Chemical	90310
T0901317	Cayman Chemical	71810
BrdU	US Biological	B2850
Tamoxifen	Cayman	13258

REAGENT or RESOURCE	SOURCE	IDENTIFIER
Citrisolv	Decon Labs	1601
Fatty acid-free bovine serum albumin	Sigma	A8806
Bovine serum albumin	AmericanBio	AB01088
HBSS	Gibco	14185–052
Collagenase Type II	Worthington Biochemical	LS004174
Phosflow Lyse/Fix Buffer	BD Biosciences	558049
DNase I	Worthington Biochemical	LS002007
Intracellular Staining Permeabilization Wash Buffer	Biolegend	421002
Isoflurane	Covetrus	11695067772
DMEM	ATCC	30–2002
FBS	ATCC	30–2020
Insulin	Sigma	I1882
IBMX	Millipore Sigma	I15879
Dexamethasone	Millipore Sigma	D4902
Oil Red O	Electron Microscopy Services	26503–02
Lipofectamine 2000 Transfection Reagent	LifeTechnologies	11668019
OptiMEM	LifeTechnologies	31985070
Protease Inhibitor	Millipore Sigma	11697498001
Phosphatase Inhibitor	Millipore Sigma	4906845001
Sample Reducing Agent	Thermo Fisher Scientific	NP0009
NuPage 2x Sample Buffer	Thermo Fisher Scientific	NP0007
TRIzol Reagent	Thermo Fisher Scientific	15596018
DAPI Fluoromount-G Mounting Media	Southern Biotech	0100–20
Wortmannin	Cayman Chemical	10010591
60% Lard High-Fat Diet	Research Diets	D12492
58% Coconut High-Fat Diet (Sucrose)	Research Diets	D12331
58% Coconut High-Fat Diet (Cornstarch)	Research Diets	D12330
43% Milk RD Western Diet	Research Diets	D12079B
45% Lard High-Fat Diet	Research Diets	D12451
45% Olive Oil High-Fat Diet	Research Diets	D06022403
45% Coconut Oil High-Fat Diet	Research Diets	D05122301
45% Fish Oil High-Fat Diet	Research Diets	D07081501
45% Safflower Oil High-Fat Diet	Research Diets	D02062102
45% Butter High-Fat Diet	Research Diets	D06022405
45% Cocoa Butter High-Fat Diet	Research Diets	D11112703
45% High Oleic Sunflower Oil High-Fat Diet	Research Diets	D07062503
45% High Oleic Safflower Oil High-Fat Diet	Research Diets	D05122103
45% Soybean Oil High-Fat Diet	Research Diets	D05042003
45% Peanut Oil High-Fat Diet	Research Diets	D16010705
Chow Diet (SD)	Harlan Laboratories	2018S
Critical commercial assays		
Cignal LXR Reporter Kit	Qiagen	336841

REAGENT or RESOURCE	SOURCE	IDENTIFIER
Alexa Fluor 594 Tyramide SuperBooster Kit, goat anti-rabbit IgG	ThermoFisher	B40944
Luciferase Assay System	Promega	E1500
Direct-zol RNA Miniprep Kit	Zymo	R2052
High Capacity Reverse Transcript Kit	Thermo Fisher Scientific	4368813
SYBR FAST Quantitative PCR Kit	Kapa Biosystems	KK4611
Pierce BCA Protein Assay Kit	Thermo Fisher Scientific	NP0007
SuperSignal West Pico Chemiluminescent Substrate	Thermo Fisher Scientifc	34577
EasySep PE Positive Selection Kit	Stem Cell Technologies	17684
Mouse Insulin ELISA kit	ALPCO	80-INSMS-E01
Deposited data		
Bulk RNA-seq of male and female APCs	GEO	Female APCs- GSE209663 Male APCs- GSE273569
Bulk RNA-seq of 3T3-L1 cells	GEO	GSE273735
Experimental models: organisms/strains		
C57BL/6J	Jackson Laboratory	000664, RRID:IMSR_JAX:000664
B6.129(Cg)-Gt(ROSA)26Sortm4(ACTB-tdTomato,-EGFP)Luo/J	Jackson Laboratory	007676, RRID:IMSR_JAX:007676
B6.129-Tg(Adipoq-cre/Esr1*)1Evdr/J	Gift from Dr. Evan Rosen, available from Jackson Laboratory	024671 RRID: IMSR_JAX:024671
Akt2 −/−	Jackson Labs	RRID:IMSR_0006966
LXRα S196A	Gage et al.[44]	https://doi.org/10.1073/pnas.1721245115
Gpr40 −/−	Latour et al.[37]	RRID:MGI:3713765
Gpr120 −/−	Bjursell et al.[36]	https://doi.org/10.1371/journal.pone.0114942
3T3-L1	ATCC	CL-173, RRID:CVCL-0123
Software and algorithms		
BD FACSDiva Software	BD Life Sciences	
CellProfiler	Carpenter et al.[101]	https://doi.org/10.1186/gb-2006-7-10-r100
Ingenuity Pathway Analysis	Qiagen	https://www.qiagenbioinformatics.com/products/ingenuitypathway-analysis
FlowJo Software v 10.1.1	BD Life Sciences	
Prism version 9.3.1	GraphPad	
TopHat	Trapnell et al.[102]	https://doi.org/10.1093/bioinformatics/btp120
HTSeq package	Anders et al.[103]	https://doi.org/10.1093/bioinformatics/btu638
DESeq2	Love et al.[104]	https://doi.org/10.1186/s13059-014-0550-8
Other		
40 μm filter	BD Falcon	352340